SPIRou :
scientific rationale

Prepared by	**Date**
JF Donati, X Delfosse, E Artigau, R Doyon	**2014 Apr 11**
Approved and accepted by	**Date**

KEY WORDS – SUMMARY

Summary	SPIRou is a nIR spectropolarimeter/velocimeter proposed as a new-generation CFHT instrument mostly aimed at **detecting & characterizing Earth-like planets in the habitable zone of low-mass stars** and at investigating how **magnetic fields impact star/planet formation**. We present here a detailed science case describing thoroughly the various science topics that SPIRou will tackle with unprecedented precision, and in particular the foremost ones for which SPIRou is expected to be world-leader. As a conclusion, we list the scientific specifications needed to tackle these issues, with a special emphasis on the need for observing in the K band and in polarized light.
Keywords	exoplanets, low-mass stars, star & planet formation, magnetic fields, precision radial velocities, spectropolarimetry, near infrared

VERSIONS

Issue	Rev.	Date	Modified pages
1	0	2013 Sep 06	Preliminary FDR version, revised from PDR version
1	1	2014 Apr 11	FDR version

DISTRIBUTION LIST

science group	CFHT
project team	

REFERENCE DOCUMENTS

N°	Name	Reference – Version

TABLE OF CONTENTS

1. General

1.1. Scope & coverage

SPIRou is a **near-infrared** (nIR) **spectropolarimeter/velocimeter** proposed as a new-generation instrument for CFHT. This document presents a detailed science case describing the multiple topics that SPIRou can tackle with unprecedented precision, and in particular the foremost ones for which SPIRou is expected to be world-leader: hunting & characterizing habitable exo-Earths around low-mass stars on the one hand (Sec 3), and investigating magnetized star/planet formation on the other hand (Sec 4).

This document also includes a list of the specifications associated to these science goals (in Sec 8) and outline (in Sec 9) the worldwide unique observational performances & opportunities that SPIRou will provide to the CFHT community.

1.2. Glossary

CFHT	Canada-France-Hawaii Telescope
RV	radial velocity
AU	astronomical unit
cTTS	classical T Tauri star
nIR	near infrared
SPIRou	spectopolarimètre infrarouge
LMS	low-mass star ($M < 0.7\ M_\odot$)
vLMS	very low-mass star ($M < 0.2\ M_\odot$)
BD	brown dwarf ($M < 0.08\ M_\odot$)
MaPP	magnetic protostars & planets
MagIcS	magnetic investigation of various classes of stars
LP	large program
ISM	interstellar medium
ALMA	Atacama large millimeter array
MHD	magneto-hydro dynamics
MRI	magneto-rotational instability
ONC	Orion nebula cluster
HZ	habitable zone
ADC	atmospheric dispersion corrector
TAC	time-allocation committee
QSO	queue service observing
S/N	signal-to-noise ratio
SED	spectral energy distribution
PAH	polycyclic aromatic hydrocarbon
YSO	young stellar object
RGB	red giant branch
AGB	asymptotic giant branch
APOGEE	Apache Point observatory galactic evolution experiment
HJ	hot Jupiter
AGN	active galactic nucleus
ELC	emission line cluster

2. Brief overview of all scientific drivers

The science programs SPIRou proposes to tackle are **forefront** (first priorities for most research agencies worldwide), **ambitious** (competitive & complementary with science programs carried out on much larger facilities, e.g., ALMA/ESO & JWST/NASA) and **timely** (ideally phased with complementary instruments, e.g., TESS/NASA, CHEOPS/ESA & JWST/NASA).

SPIRou plans to concentrate on two main scientific goals. The first one is to **search for & characterize habitable exo-Earths orbiting low-mass & very-low mass stars** (LMSs & vLMSs) using high-precision radial velocity (RV) measurements. This search will expand the initial, exploratory studies carried out with visible instruments (e.g., HARPS/ESO) and will survey in particular large samples of stars mostly out of reach of existing instruments. In particular, carrying out a new large-scale survey at nIR wavelengths will boost the sensitivity to habitable exo-Earths by typically an order of magnitude on planetary mass (with respect to existing instruments). SPIRou will also work in close collaboration with space- & ground- based photometric transit surveys like K2/NASA (new mission concept for Kepler, to be decided in 2014), TESS/NASA, CHEOPS/ESA, ExTrA[1] and PLATO/ESA (after being launched in 2024) to identify the true planets among the candidates they will discover.

The second main goal is to **explore the impact of magnetic fields on star & planet formation**, by detecting fields of various types of young stellar objects (e.g. class-I, -II and -III protostars, young FUor-like protostellar accretion discs) and by characterizing their large-scale topologies. SPIRou will also investigate the potential presence of giant planets around protostars and in the inner regions of accretion discs. In particular, this study will vastly amplify the initial exploration surveys carried out at optical wavelengths within the MaPP (Magnetic Protostars and Planets) and MaTYSSE (Magnetic Topologies of Young Stars and the Survival of close-in massive Exoplanets) CFHT Large Programs (LPs). It will also ideally complement the data that ALMA/ESO has just started collecting on outer accretion discs & dense prestellar cores.

SPIRou will also be able to tackle many additional exciting research topics in stellar physics (e.g., dynamos of fully convective stars, weather patterns of brown dwarfs), in planetary physics (e.g., winds & chemistry of solar-system planets), galactic physics (e.g. stellar archeology) as well as in extragalactic astronomy.

We detail these goals below (Secs 3-7), giving in the main cases the typical samples that need to be explored & their observational properties; the estimated observing times for the various programs are also summarized in Appendix B. From this, we derive the scientific specifications of SPIRou & their relative importance for the various research topics and in particular for the two main goals (Sec 8). We finally outline (Sec 9) that SPIRou will provide a **worldwide-unique opportunity** of tackling the aforementioned science issues with maximum efficiency.

[1] ExTrA is a recently funded ERC project (w/ X.Bonfils as PI) whose aim is to detect transiting Earth-like planets around M-dwarfs from the ground. As a low resolution multiple-object spectrograph, ExTrA will allow extremely accurate photometry in narrow wavelength bands

3. Detecting exoplanets around low-mass dwarfs

3.1. Context

One of the most exciting areas of astronomical research today is the study of exoplanets & exoplanetary systems, engaging the imagination not just of the astronomical community but of the general population. Since the pioneering discovery of a giant planet around 51 Peg (Mayor & Queloz 1995, Nature 378, 355), about 1,000 extra-solar planets have now been detected, revolutionizing planetary science by placing our unique solar system into a much broader context. More specifically, these discoveries allow us to **explore the surprising diversity of planets and planetary systems**, and to **investigate the physical processes through which they form**; for instance, they demonstrate the crucial role of planet migration in the formation process, even in the case of our own solar system. There is now a tremendous interest for **studying Earth-mass rocky planets**, in particular those **located within the habitable zones (HZs) of their host stars**, i.e., in the orbital range where liquid water can be stable at the planetary surfaces. Identifying habitable Earth-like planets and searching for biomarkers in their atmospheres is among the main objectives of this new century's astronomy, motivating ambitious space missions (JWST/NASA, TESS/ NASA, CHEOPS/ESA, PLATO/ESA)

The majority of the exoplanets now known were discovered thanks to RV studies measuring Doppler shifts induced by orbiting planets in the spectrum of their host stars. Astronomical instrumentation has progressively matured to the level where it is now possible to detect terrestrial planets orbiting distant stars, with the most stable visible-light spectrograph reaching a RV precision of <1 m/s (i.e., HARPS/ESO). Although quite a spectacular achievement, this performance is still at least an order of magnitude away from the precision needed to detect an Earth analog orbiting a Sun-like star. Other techniques for detecting candidate exoplanets include photometric monitoring of eclipses from planets transiting in front of their host stars, requiring ultra-high photometric precision for detecting Super-Earth-like planets that only space probes (e.g., CoRoT/CNES, Kepler/NASA) can achieve today for Sun-like stars.

Much interest has recently been focused on low-mass M dwarfs, around which habitable super-Earths are much easier to detect. To simplify the search for distant terrestrial planets, an alternative is to study the cooler, less massive, much more numerous red & brown dwarfs whose RV curves are comparatively more sensitive to the presence of exoplanets. Low-mass dwarfs vastly dominate the stellar population (8 of 9) in the solar neighborhood and are likely hosting most planets in our Galaxy (Bonfils et al. 2013, A&A, 549, 109). Moreover, their reduced temperatures move their HZs closer in, further increasing RV signals from exoplanets potentially orbiting therein (see Tab 3.1): this is how the first potentially habitable super-Earth (~5-7 times as massive as our Earth) was discovered around a 0.3 $M_\odot$ M4 star (Gl 581, Udry et al 2007, A&A 469, L43; Mayor et al 2009, A&A 507, 487; see Fig 3.1) and how most potentially habitable super-Earths known as of today were discovered around M-dwarfs (Gl667Cc Bonfils et al 2013, A&A 549, 109; Delfosse et al 2013, A&A 534, 8; Gl163c Bonfils et al 2013, A&A 556, 110).

Similarly, photometric transits of M dwarfs are deeper for a given planet radius (scaling as $1/R_\star^2$, with $R_\star$ noting the stellar radius) and thus easier to observe from the ground (e.g., Charbonneau et al 2009, Nature 462, 891; Bonfils 2012, A&A 546, 27; see also Fig 10 of Winn 2010, astro-ph:1001.2010). A prime goal of the coming years

Fig 3.1: Artist view of the 4-exoplanet system orbiting the red dwarf Gl 581 (© ESO)

is to discover Earths or super-Earths whose atmosphere can be scrutinized and characterized with future space missions (such as JWST/NASA and possibly later-on by EChO/ESA). Since atmospheric characterization primarily requires as deep an atmospheric transit as possible on the one hand, and as bright a star as possible on the other hand (in the nIR, where absorption from atmospheric molecules mostly concentrates), M dwarfs are optimal targets for this quest (Rauer et al 2011, A&A 529, 8). Today, only a handful of very-bright transiting systems have been discovered up to now - most being giant gaseous planets.

Given their low temperatures, red & brown dwarfs are much more accessible at nIR wavelengths (see Fig 3.2 and Tab 3.2). **High-resolution nIR spectroscopy accurate to the 1 m/s level**, yielding **wide simultaneous spectral coverage** (not yet available on any telescope worldwide) therefore appears as optimal for carrying out systematic RV surveys of M & L dwarfs aimed at investigating the statistical properties of exoplanetary systems. With additional **spectropolarimetric capabilities**, one can simultaneously investigate magnetic fields and activity of all surveyed dwarfs and filter out RV curves (at least partially) from activity-induced non-planetary signals, giving a wider access to lower mass dwarfs (more active on average).

The various front-line exoplanet science programs that can strongly benefit from such observations, as well as the associated feasibility issues, are discussed below in more details.

3.2. A nIR search for habitable exo-Earths around M dwarfs

Discovering habitable Earth-like planets and searching for biomarkers in their atmospheres are amongst the main objectives of this new century's astronomy and motivate reflexion around very ambitious future space missions such as Darwin/ESA & TPF/NASA. However, much can (and must) be learned prior to the launch of such missions, e.g., how frequent terrestrial planets are and which fraction lie in the HZ, what type of planets can be found there, and around which type of stars they mostly occur. Ideally, one would need to complete a pre-launch catalog of habitable terrestrial planets, allowing future space missions to concentrate on planet characterization without wasting time on detection. It is therefore crucial to determine

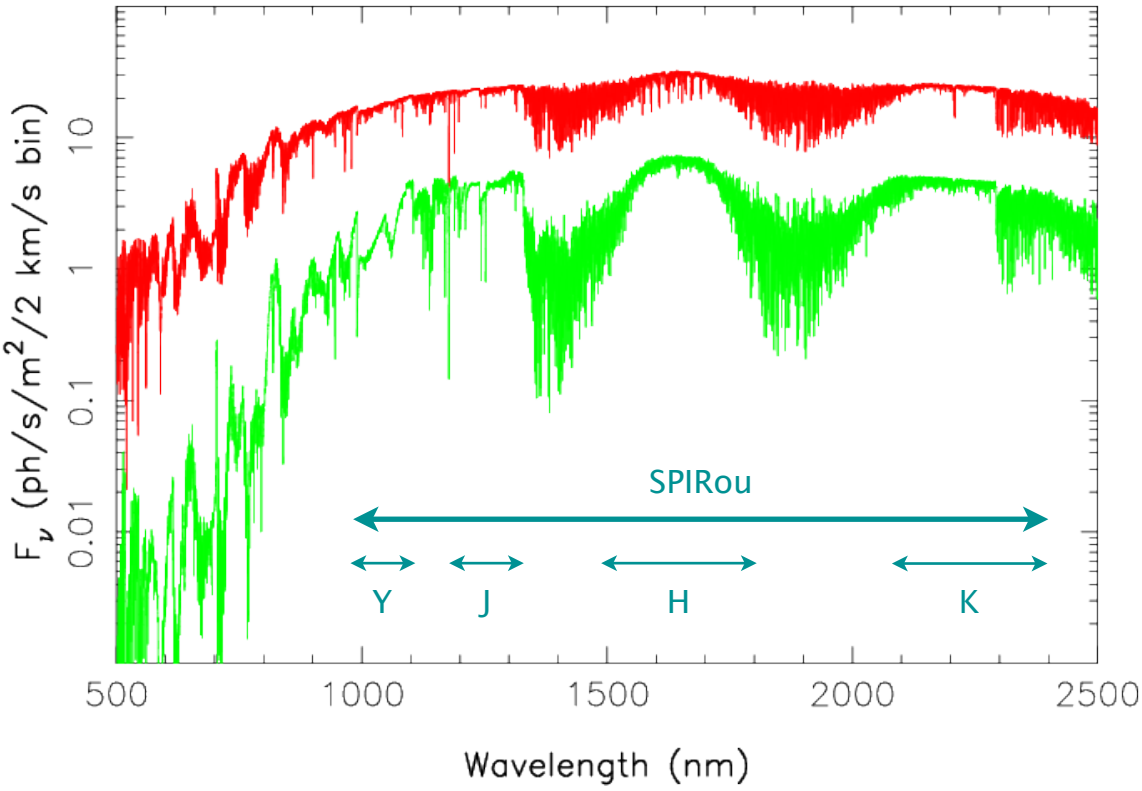

Fig 3.2: Photon distribution (per 2 km/s velocity bin size) for a M6 (3,100 K, red) and M8 (2,300 K, green) dwarfs @ 10pc (derived from NextGen models, Allard et al 1997, ARA&A 35, 137). M6 and M8 dwarfs respectively produce ~30 and ~1000 times more photons (per velocity bin) in HK than in V.

how frequent and where habitable exo-Earths are in the solar neighborhood and to **start characterizing their physical properties**.

JWST/NASA and possibly EChO/ESA will have the capacity to characterize Earth- or super-Earth-type planet atmospheres prior to the more ambitious future space missions such as Darwin/ESA or TPF/NASA. However, their limited sensitivity will only allow them to focus on transiting planets around bright stars, mainly M-dwarfs in the solar neighborhood (see Sec 3.2). The search for transiting planets in the HZs of close M-dwarfs has thus become one of the main quests in exoplanet research.

Ground based high-precision RV programs (e.g., with HARPS/ESO, Mayor et al 2009, A&A 507, 487) have initiated this task. The space-based photometric missions CoRoT/CNES and Kepler/NASA allowed to detect a few transiting exo-Earths. However, since these missions were limited to a small region of the sky, these targets are too faint for future atmospheric characterization, e.g., with JWST/NASA; moreover, the number of confirmed exo-Earths detected around bright stars remain very small[2]. Only ground-based high-precision RV velocimeters (e.g., SPIRou/CFHT in the nIR, HIRES-ESPRESSO/ESO in the visible on a limited sample) and forthcoming space-based

[2] Among all candidate exoplanets detected with Kepler, most are too faint for spectroscopic and RV follow-ups, with only a few true exo-Earths (at most – not to mention their habitability) to be found among the brightest candidates. Even if Kepler has some intrinsic ability to exclude false detections, e.g., caused by background eclipsing binaries (e.g., Torres et al 2011, ApJ 727, 24), the rate of false positive rate is nevertheless significant, ~35% for Giant planet and ~10% for Super-Earth (Santerne et al 2012, A&A 545, 76). RV measurements are thus mandatory to derive exoplanet masses and thus obtain definite confirmation that detected planets are true exo-Earths. About 90 Kepler planet candidates smaller than Neptune were detected around M-dwarfs (Dressing & Charbonneau 2013, ApJ 767, 95), including 2 candidates in the HZ. Unfortunately, these 2 candidates orbit stars to faint to secure precise RV measurements.

Table 3.1: Typical properties of late-M dwarfs, including the location & extent of their habitable zones, the corresponding range of rotation periods, the RV semi-amplitude $K_\oplus$ & $K_{5\oplus}$ expected from habitable planets of masses 1 & 5 $M_\oplus$ (the full RV variation being 2x larger) and the maximum depth of photometric transits from Earth-size planets. Green/pink figures outline cases where 60 RV measurements @ 1 m/s precision can yield definite/marginal detections respectively (see Fig 3.10 for the detection probability as a function of the number of measurements).

ST	M ($M_\odot$)	R ($R_\odot$)	T (K)	HZ (AU)	Prot (d)	$K_\oplus$ (m/s)	$K_{5\oplus}$ (m/s)	ΔM (mmag)
Sun	1	1	5780	0.8-2.0	260-1000	0.1	0.5	0.08
M4	0.30	0.30	3400	0.10-0.28	24-100	0.4	2	0.9
M6	0.13	0.15	3000	0.04-0.12	9-40	0.8	4	3.6
M8	0.08	0.10	2300	0.008-0.02	1-4	3	15	8

photometers (e.g., TESS/NASA to be launched in 2017; PLATO/ESA to be launched in 2024) will be able to expand the search, in a collaborative way (see e.g., Sec 3.3), to many more nearby (and brighter) stars. In the meantime, there is a crucial need for surveying as large a fraction of the sky as possible, and in particular the immediate solar neighborhood.

As TESS/NASA will operate on 27-d windows of continuous monitoring for most stars, the majority of planet candidates showing at least 2 transits will have periods <20 d and will not be located in the HZ of their host stars. For planets with longer periods, and in particular for those located in the HZ, RV-driven planet searches will be more efficient. Photometric follow-ups of all planets detected with RV surveys may be achieved once their ephemeris is sufficiently well known to determine accurately the time window of the potential transit (see for example Bonfils et al 2012, A&A 564, 27). While PLATO/ESA should have the potential to discover transiting Earth-like planets with longer periods than TESS/NASA, its late launch (>2024) will not allow to provide targets to JWST/NASA, at least for the first ~6 years of operation.

To be considered as potentially habitable, a planet should be within the right range of distances from its host star (and thus in the right range of temperatures) to allow water on its surface to be stable in the liquid state; the atmospheric pressure at the planetary surface should also be lower than the critical value above which liquid water cannot exist[3]. The transition between Earth-like planets (dominated by a rocky or icy core) and Neptune-like planets (with a massive H-He gas envelope surrounding the core) is usually placed at ~10 $M_\oplus$, although this is more of an educated guess than a quantitative estimate. We consider here that habitable planets should have masses in the range 0.5-10 $M_♁$. Note that the distances and orbital periods which correspond to the HZs strongly depend on the mass of the host star (e.g., Selsis et al. 2007 A&A 476, 1373, see also Figs 3.3 and 3.4 and Tab 3.1).

The brute-force strategy to detect habitable rocky planets is to search for Earth clones, i.e., planets of at most a few Earth masses with orbital periods of 0.9-2 yr, around Sun-like stars. This, however, requires the development of ultra-stable spectrographs (accurate to a few cm/s over several years, e.g., HIRES-ESPRESSO/ESO)

[3] Other criteria are often invoked in the literature to argue about the habitability of exoplanets, like for instance the potential impact of increased flaring from the host star and synchronization of the planet rotation with its orbital motion. Both issues are essentially speculative & controversial (e.g., Segura et al 2010, AsBio 10, 751) and mostly relevant to astrophysical domains that are still largely in their infancy (e.g., exo-planetology, exo-climatology, exo-biology). We therefore do not include them in the definition of an habitable planet (until at least there is a clear consensus on the subject) and thus keep the more traditional and secure definition given in the text. See Appendix C or Delfosse et al. (2013, A&A 553, 8) for a more extensive discussion.

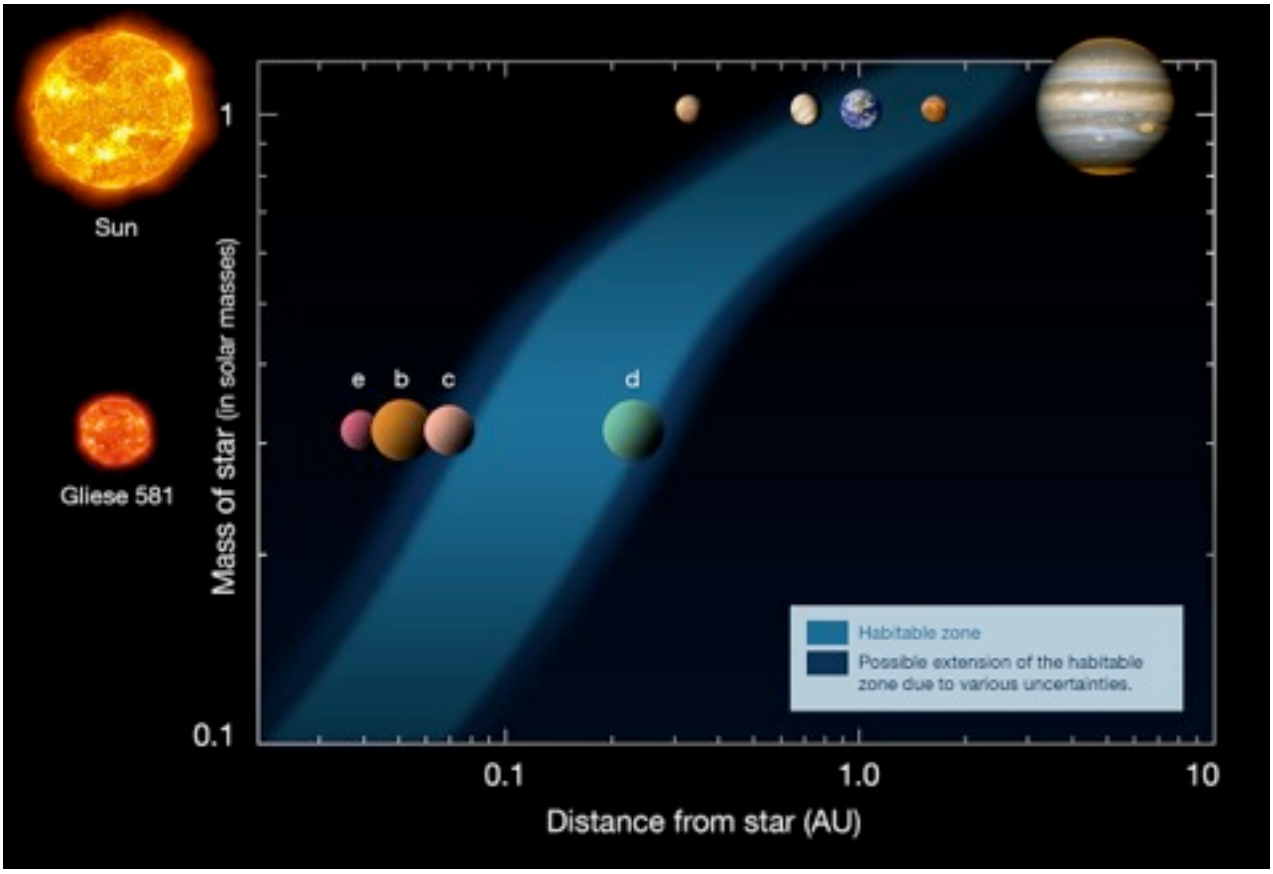

Fig 3.3: Location of the habitable zone as a function of stellar mass. The cases of the Sun (with its 4 rocky planets and Jupiter) and the red dwarf Gl 581 (with its 4 detected exoplanets) are also included (© ESO).

or space astrometric missions (accurate to better than 1 μas). Whereas this approach must obviously be pursued, it is extremely demanding and is not technically mature yet. The faster, smarter, approach is to look for habitable planets around very-low-mass dwarfs, for which habitable exo-Earths are expected to produce comparatively larger RV wobbles - thanks to their tighter HZs (see Fig 3.3 & Table 3.1) and to the lower mass of the host star; in this case, a 1 m/s RV precision is sufficient to detect habitable telluric planets around 0.3 $M_\odot$ dwarfs, with the much shorter orbital periods (of order of weeks) greatly decreasing the measurement collection timescale.

Ongoing searches of exoplanets orbiting low-mass dwarfs are using visible high-resolution spectrographs (e.g., HARPS/ESO) and are essentially limited to the ~100 closest southern red dwarfs more massive than ~0.3 $M_\odot$ (i.e., to spectral types earlier than M4). Lower-mass or more distant dwarfs are simply too faint for visible surveys at a RV precision of 1m/s, and **can only be investigated in the nIR** where their photons distributions peak, e.g. exceeding those in the visible by ~1000x for an M8 star (see Fig 3.2 and Tab 3.2). Given that chances of detecting habitable super-Earths with HARPS/ESO within the surveyed early M-dwarfs were <10% (as a result of the limited sensitivity and coverage, Bonfils et al 2013, A&A 549, 109), the few detections obtained on a sample of 100 dwarfs strongly suggest that these objects are potentially very frequent around very-low-mass stars, with an occurrence rate of 41^{+54}_{-13}%. Similarly, from Kepler detections, few teams derive an occurrence rate of Earth-size habitable planets around M dwarfs varying between 46^{+18}_{-15}% and 66^{+25}_{-13}% (Gaidos 2013, Kopparapu 2013 ApJ 767, L8; Dressing & Charbonneau in prep). The difference between both estimates been mostly attributable to low-number statistics and to the slight difference in the considered samples. **It demonstrates that time is ripe for**

determining accurately how frequent habitable Earth-like planets are around M dwarfs, for finding out those in the solar neighborhood and for characterizing their physical properties.

The RV impact of habitable Earth-like planets of masses 0.5-10 $M_\oplus$ is shown in Fig 3.4 for different masses of host dwarfs; a RV semi-amplitude (K) of >1 m/s is produced by habitable planets of >3 $M_\oplus$ around 0.3 $M_\odot$ (M4) dwarfs, and of >1 $M_\oplus$ around 0.1 $M_\odot$ (M7) dwarfs. **A stability of 1 m/s is thus mandatory for detecting habitable Earth-like planets around mid- and late-M dwarfs.** At a degraded RV prevision of ~3 m/s, habitable super Earths (<10 $M_\oplus$) can no longer be detected around 0.3 $M_\odot$ dwarfs; with the RV precision further degraded to ~10 m/s, only massive habitable super-Earths (>7 $M_\oplus$) around early-L dwarfs can be detected and no habitable super-Earths can be detected around mid- and late-M dwarfs. Monte Carlo (MC) simulations (detailed in Sec 3.8) further demonstrate that practically all habitable planets of mass <7 $M_\oplus$ remain undetected at a degraded RV precision of 3 m/s. Our MC simulations also indicate that a planet featuring K=1 m/s has a 80% probability to be detected with 60 RV measurements at a precision of 1m/s (see Sec 3.8).

Low mass stars feature a rich nIR spectrum with thousands of atomic and molecular lines whose strengths increase at lower temperatures, ensuring that RV wobbles induced by Earth-like rocky planets are detectable; estimates of RV precision from synthetic nIR spectra (with a resolving power of ~75,000 and a S/N of ~160 per 2 km/s pixel) indeed suggest that a **RV precision of ~1 m/s is attainable for mid to**

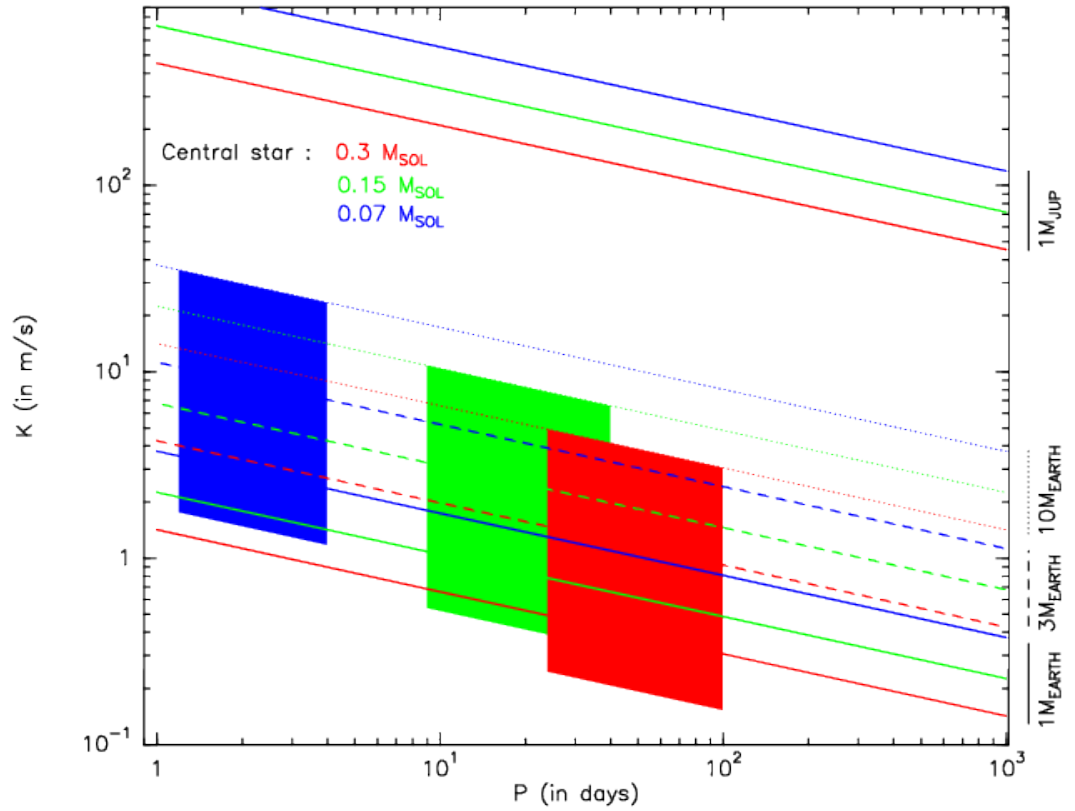

Fig 3.4: Radial velocity semi-amplitude K (in m/s) of the reflect motion induced by a planet on its host dwarf as a function of the planet orbital period P (in d), for planet masses of 1 $M_\oplus$ (full lines, bottom), 3 $M_\oplus$ (dashed lines), 10 $M_\oplus$ (dotted lines) and 1 $M_\oplus$ (full lines, top) and for host dwarf masses of 0.3 $M_\odot$ (red), 0.15 $M_\odot$ (green) and 0.07 $M_\odot$ (blue) - corresponding respectively to M4, M6 and early-L dwarfs. The red, green and blue parallelograms illustrate, for each dwarf mass, the RV impact of 0.5-10 $M_\oplus$ planets within the HZs, i.e. with orbital periods of 24-100 d, 9-40 d and 1-4 d for 0.3 $M_\odot$, 0.15 $M_\odot$ and 0.07 $M_\odot$ dwarfs respectively.

Table 3.2: Number of solar neighbourhood M-dwarfs that can be measured with a RV precision of 1m/s or 3 m/s for exposure time varying between 5 and 60 minutes. The numbers of M0-M6 dwarfs are extracted from the Lépine et al catalog (2011, AJ 142, 138) whereas the number of M7-M9 dwarfs are obtained by extrapolating the 15pc sample to larger distances.

ST	M0	M1	M2	M3	M4	M5	M6	M7	M8	M9
# of stars w/ J<8.3 (1m/s RV in < 5 min)	325	185	165	155	100	20	10	1	1	1
# of stars w/ 8.3<J<9.5 (1m/s RV in 5-15 min)	800	655	485	540	525	160	35	12	4	2
# of late-M w/ J<11.9 (3m/s RV in < 15 min)								30	16	3
# of late-M w/ 11.9<J<13.4 (3m/s RV in 15-60 min)								240	125	23

late M dwarfs, with spectral lines from the K band being the main contributors to the final RV precision (see Sec 8).

The ambitious, though realistic, **planet search we propose with SPIRou aims at monitoring a sample of ~600 M-dwarfs, performing in average ~55 visits per star** (with S/N~172 spectra per visit to reach an accuracy of 1m/s) **and requiring in total 600 observing nights.** Our MC simulations indicate that the SPIRou planet search would detect ~450 planets, including ~300 with masses <5 $M_\oplus$ and ~55 of them lying in the HZ. Fig 3.5 illustrates one realization of these MC simulations (see details on the technical implementation in Sec 3.8) with detected / undetected planets shown in a mass/temperature diagram. The lower envelope of detected planets ranges from 2 to ~0.4 $M_\oplus$ depending on temperature, and the survey is more than 50% complete above 200K and 2 $M_\oplus$. A planet search such as that we propose would provide a drastic (10-fold) improvement in the number of known, e.g., hot-sub-Earths or transiting habitable planets - populations for which we only have low-number statistics at the moment. The catalog of the SPIRou planet search will be finalized later on, and will be optimized as our knowledge on planets around M dwarfs progresses.

Photometric follow-up of all planets detected with SPIRou will be achieved with CHEOPS/ESA and ExTrA, to determine which are transiting once their ephemeris and transit windows are well known. Our MC simulations indicate that this survey should statistically detect ~2 transiting Earth-like planets in the HZ, as well as 10-20 transiting Earth-like planets orbiting closer-in (see Fig 3.5). These objects will be prime targets for space missions dedicated to atmospheric characterization, starting with JWST/NASA.

One representation of a «discovery phase» of the SPIRou survey could consist in observing the **360 M dwarfs** with the highest planet detectability. This initial survey will help refining the observing strategies of the larger survey. **It can be completed within 300 observing nights**. MC simulations demonstrate that this survey would detect ~290 planets, including ~200 with masses <5 $M_\oplus$ and ~35 of them lying in the HZ. **This 360-dwarf SPIRou discovery survey would allow to determine the frequency of habitable Earth-like planets around M dwarfs $\eta_\oplus$ to an accuracy of ~12%, while the full planet search will further improve this accuracy to better than 10%.** By breaking down the full stellar sample in 0.5-dex bins in orbital period and mass, the proposed 360-dwarf discovery survey would provide occurrence rates of Earth-like planets in each mass / period bin with a ~20% accuracy (see Figure 3.6). The proposed survey will also probe, for the first time in RV studies, the occurrence rate of sub-Earth-mass planets with orbital periods shorter than ~10 days. The recent

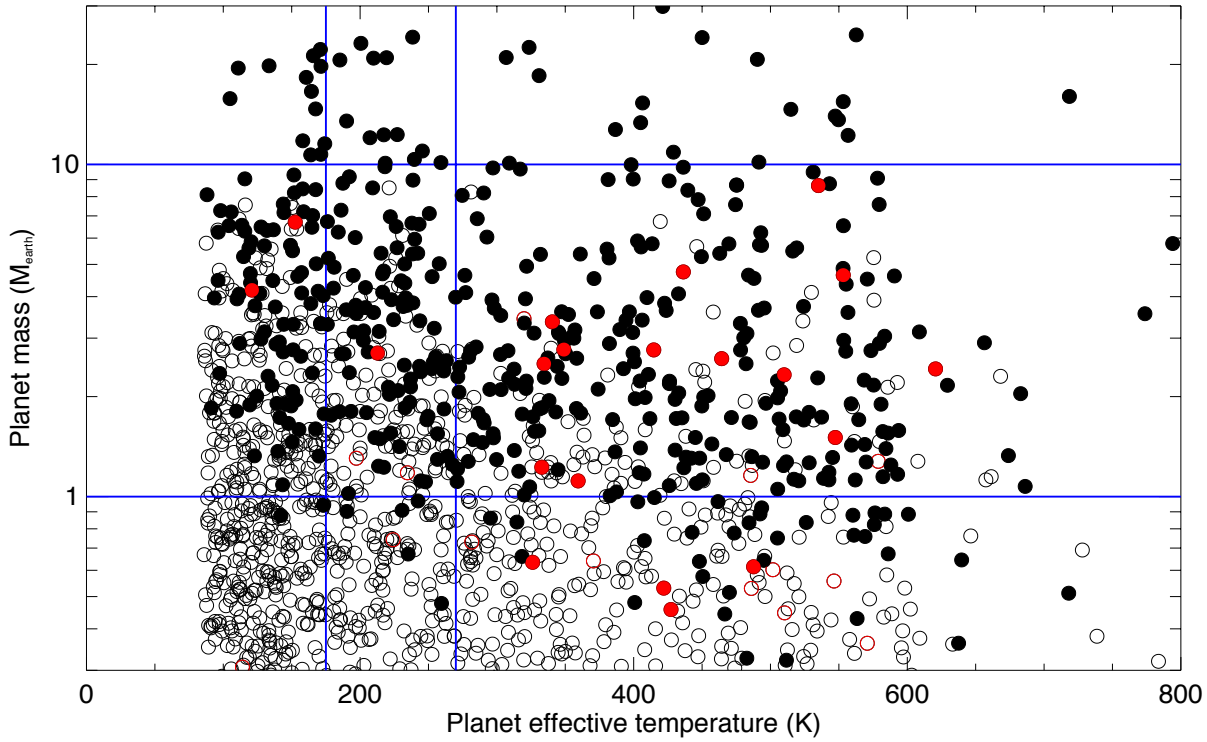

Fig 3.5 : Planets found with the 600-target survey. Filled circled indicate detected planets, open circles undetected ones and red circles (both filled and open) represent transiting planets. Blue lines show notional limits for the habitable zone, both in mass and temperature. Most planets with >2M⊕ in the habitable zone are detected, including one transiting. Interestingly, a sample of sub-M⊕ planets with >350 K is also detected.

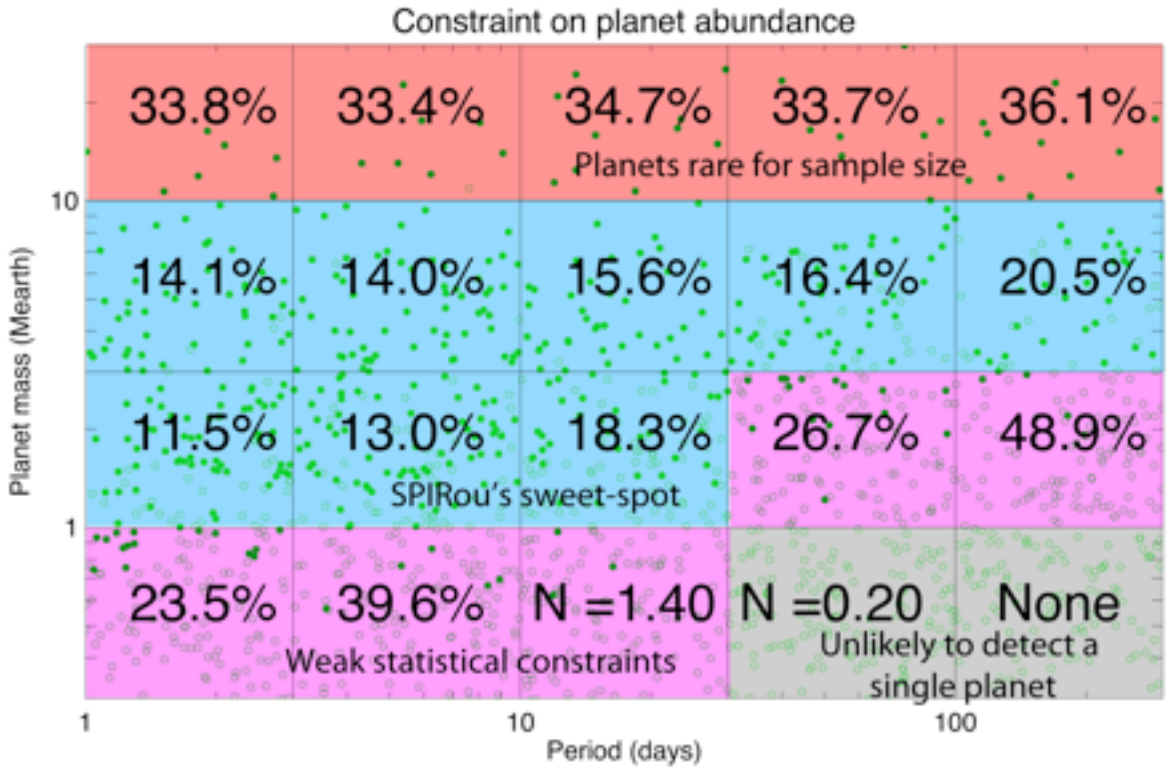

Fig 3.6: Constraints on the abundance of planets for different period and mass bins for the 360-star SPIRou discovery survey. The quoted uncertainties are assumed to be purely due to Poisson noise. For bins where fewer than 2 objects are expected, we simply indicate the expected number. A 20% accuracy on the abundance corresponds to 25 objects found within the bin. The background circles indicate the detections and non-detections (filled and open circles) for an arbitrarily selected MC realization.

discovery of the KOI-961 system, with 3 Mars-sized planets in close orbit around an M5 dwarf among the very small sample of late-Ms in the Kepler field, indicates that such worlds are likely to be very common (Muirhead et al 2012, ApJ 747, 144). Furthermore, the very tight orbits of these planets leads to high probabilities of transit (~10% for each planet in that part of the diagram).

By 2017, the number of known habitable super-Earths should still be small; **only large surveys such as the SPIRou planet search we propose and its discovery phase can provide a large enough number of detections to carry out a proper characterization of habitable super-Earths**.

3.3. Transiting close-in exoplanets

Exoplanets transiting their host stars are especially interesting as **sensitive probes of their internal structures and atmospheres** (Charbonneau et al 2007, PPV). The planets transiting around bright stars are indeed the only ones whose masses (through RV monitoring of their orbital motion) and radii (through photometric monitoring of their transits) can be measured simultaneously, allowing one to estimate their densities and internal composition. When the host star is bright enough, transiting planets can even tell us about the composition & physics of their atmospheres, opening the new research field of exo-planetology (see Sec 6.3). Only a handful of very-bright transiting systems have been discovered up to now, most of them being giant gaseous planets.

A prime goal of the coming years is to discover Earths or super-Earths whose atmosphere can be scrutinized and characterized with future space missions such as JWST/NASA and possibly EChO/ESA (see Sec 6.3). Since atmospheric characterization primarily requires as deep an atmospheric transit as possible on the one hand, and as bright a star as possible on the other hand (in the nIR, where absorption from atmospheric molecules mostly concentrates), M dwarfs are optimal targets for this quest. Detailed simulations show that atmospheric components of Earth-like extrasolar planets will produce a detectable signal for planets around M dwarfs planets using JWST/NASA and /or ELTs, but not for similar planets around Sun-like stars (e.g., Rauer et al 2011, A&A 529, 8; Tinetti et al 2012, ExA 34, 311). Fig 3.7 depicts all known transiting planets as a function of the two main parameters characterizing the suitability of an atmospheric follow-up : IR brightness and transit depth (of an annular equivalent to 1 atmospheric scale height). Only three Neptune-size/Super-Earth planets are actually characterizable, all located around M-dwarfs (namely GJ 436, GJ 1214 and GJ 3470; Gillon et al 2007, A&A 472, L13; Charbonneau et al 2009, Nature 462, 891; Bonfils et al. 2012 A&A 546, 27 - see Fig 3.7).

Detecting candidate Earth-like planets transiting across the disc of their host stars through photometric monitoring is much easier for low-mass dwarfs, transits being comparatively deeper as a result of the smaller radii of the host dwarfs (see Table 3.1). For instance, transits of GJ 1214b (orbiting a M5 dwarf) are ~40 times deeper that those of CoRoT-7b (orbiting a G9 star, see Fig 10 of Winn et al 2010, astro-ph:1001.2010). The photometric quest for transiting super-Earths around dwarfs has already started from the ground (e.g., Mearth focussing on M dwarfs, Irwin et al 2009, AIPC 1094, 445, or ExTrA) and from space (e.g., with CoRoT/CNES, Kepler/NASA) and should progressively become more sensitive and ambitious in the future (TESS/NASA and PLATO/ESA), aiming at planet masses & radii closer to those of the Earth. To detect habitable Earth-size planets through photometry, M dwarfs are

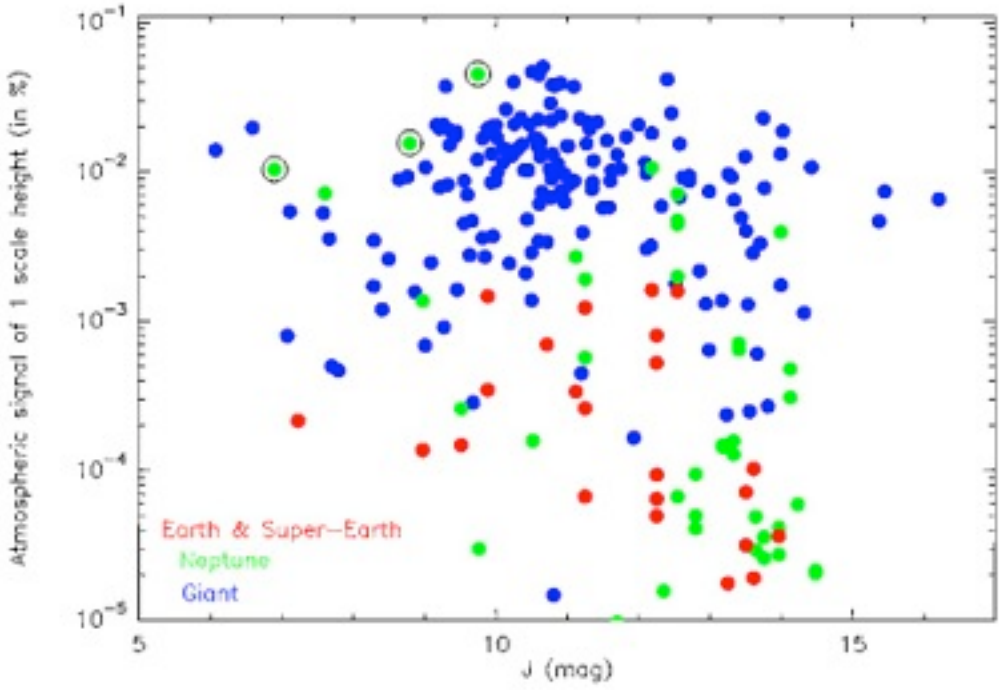

Fig 3.7: Attributes for atmospheric follow-up suitability: J-band stellar brightness and atmospheric transit depth for all the transiting planets detected to date. The best targets for atmospheric characterization are located in the top left quadrant (brightest and with deepest transits). The vast majority of them are Jupiter-like planets (in blue); only few Neptune (in green) are attainable and are mostly around M-dwarfs (black open circle). To date, no Earth-sized planet has been found in this part of the parameter space.

particularly well suited, the relatively small size of their HZs strongly increasing the probability of transits. While results from CoRoT/CNES and Kepler/NASA on this issue remain limited (see Sec 3.2), ground-based (e.g., ExTrA targeting mid to late-M dwarfs) and space-based photometers (e.g., TESS/NASA, that will survey 500,000 stars including the 1,000 closest M dwarfs from 2017) should detect ~300 transiting Earth-size planet candidates.

Ground-based nIR spectroscopy is essential to this quest; spectroscopy is indeed mandatory to establish the planetary nature of all transiting objects detected around low-mass dwarfs through photometric monitoring (and discard false detections, e.g., caused by background eclipsing binaries) and to measure their mass from the RV amplitude of their host dwarfs' orbital motion. A high-precision velocimeter working in the nIR will thus be essential to monitor all candidates detected with ground and space photometers (and in particular with TESS/NASA) around bright M dwarfs, hardly accessible to velocimeters working in the visible like HARPS/ESO (see Fig 3.2). As shown on Fig 3.4, detecting Earth-like planets around bright mid-M dwarfs at orbital periods <20 d **requires a RV precision of 1 m/s**.

TESS/NASA, to be launched in 2017, is predicted to discover ~300 transiting super-Earth candidates, most of them orbiting around M dwarfs. Since <30% of them will be accessible to optical RV follow-ups (Deming et al 2009, PASP 121, 952), **SPIRou will be the best RV instrument to monitor in the nIR the ~150 best candidates visible from CFHT** (with ~60 visits per star and with S/N~160 spectra per visit), to establish or reject their planetary nature and to determine their masses and eccentricities; **this observational effort, that we propose as a specific item of the SPIRou planet search, requires a total of 150 observing nights. In the initial**

discovery phase of our planet search, requiring 75 CFHT nights, we will mostly focus on the TESS/NASA planet candidates with smallest radii and orbits closest to their HZs. Furthermore, since Earth-like planets are very often found in multi-planetary systems, a RV follow-up of TESS/NASA candidates will likely discover other planets in the systems, especially at large orbital separations. Because planets are generally co-aligned in planetary system, such planets will have a high probability of transit and will be monitored to search for such transits (with CHEOPS/ESA or ExTrA) once the ephemeris is well known.

Using high-resolution spectroscopy, one can also estimate how tilted the orbits of transiting planets are with respect to the rotation axis of their host stars, and whether their orbital motions are prograde or retrograde, through the Rossiter-McLaughlin effect in slow rotators (e.g., Bouchy et al 2008, A&A 482, L25) or through line profile variations in more rapid rotators (Cameron et al 2010, MNRAS 407, 507). While spin-orbit alignments are often observed for Jupiter-mass planets, significant misalignments are also reported (e.g., Hébrard et al 2008, A&A, 488, 763; Moutou et al 2009, A&A, 498, L5). These misalignments potentially result from gravitational interactions with a companion or other massive planets in the system (e.g., Triaud et al 2010, A&A 524, 25), and can thus statistically document the configuration & evolution of non-solar planetary systems. A super-Earth transiting an M-dwarf typically provides a 10 m/s Rossiter-McLaughlin anomaly (provided a rotational broadening of a few km/s), that can be measured and characterized with a RV precision of 1 m/s.

3.4. Exoplanet statistics around M dwarfs

With ~1000 known exoplanets, there are now several emerging trends between the properties of the planets and their host stars. The most well known is the increase in the frequency of giant planets with the metallicity of the host star (e.g., Santos et al 2004, A&A 415, 1153). Recent RV surveys also suggest that the giant planet frequency also increases with stellar mass (e.g., Johnson et al 2007, ApJ 670, 833) while micro-lensing surveys show that low-mass planets are overabundant with respect to giant planets around low-mass stars (e.g., Gould et al 2010, ApJ 720, 1073). These trends can provide observational tests for the 2 main planet formation theories - the core-accretion model where planets form through accretion of dust and gas around solid cores (e.g., Pollack et al 1996, Icarus 124, 62) and the alternative mechanism where a relatively massive disc cools enough to fragment into small clumps through gravitational instabilities (e.g., Durisen et al 2007, PPV). Having different sensitivities to the physical conditions in the protostellar disc, both scenarios make contrasting predictions on how much gas giants and super-Earths end up being formed depending on the mass of the host star (e.g., Kennedy & Kenyon 2008, ApJ 682, 1264).

The HARPS/ESO RV survey targeting M dwarfs has been class-leading (see Bonfils et al 2013, A&A 549, 109 for a review). It is the most complete planet search program around M dwarfs to date, demonstrating in particular that super-Earths (2-10 $M_\oplus$) are frequent around M dwarfs with an occurrence rate of 88^{+55}_{-19} % (for orbital period <100 d), to be compared to ~50% for similar planets around G dwarfs. As these results are based on a very small numbers of planets, they have large statistical uncertainties (see Sec 3.2). It is noteworthy that the majority of Earth-like planets known to date have been found around M-dwarfs despite the observational challenges to observe these targets in the visible domain.

A very significant contribution to the field would be to determine more accurately the statistics of low-mass planets around early-M dwarfs, and to compare with those already found around solar-type stars. The preliminary estimate from HARPS needs to be observationally confirmed through an extensive survey of hundreds of early M dwarfs, expanding the results of the ongoing surveys carried out on visible instruments (essentially limited to the ~100 brightest early-M dwarfs within 10 pc). A typical RV precision of ~1 m/s is needed to detect >3 $M_\oplus$ planets with orbital periods <100 d around 0.3 $M_\odot$ stars (see Fig 3.4); a degraded RV precision of ~3 m/s would only allow to survey planets more massive than 10 $M_\oplus$.

The surveys proposed in Sec 3.2 and 3.3 will already provide a drastic improvement of the current situation. Moreover, by extending further the RV monitoring on a selected sample of M dwarfs with detected planets, SPIRou can reveal additional bodies in most systems and further improve statistics on multi-planetary systems. This additional monitoring can be carried out on the ~350 most interesting M dwarfs with detected planets / systems, requiring an additional amount of 250 CFHT nights to achieve 40 more visits per star.

3.5. Giant planets around ultra-cool dwarfs

Pushing further the exploration into the L-type brown dwarf regime is also expected to yield very valuable results. In particular, it should show (and yield first quantitative statistics on) how commonly brown dwarfs host planets - a yet poorly documented piece of observational information, with only a few planetary-mass companions more massive than Jupiter detected around ultra-cool dwarfs through high-angular resolution imaging (e.g., Chauvin et al 2004, A&A 425, L29) and just as few RV monitorings of ultra-cool dwarfs achieved @ a precision of 50-100 m/s (e.g., Joergens & Muller 2007, ApJ 666, L113; Blake et al 2010, ApJ 723, 684). This exploration is crucial as it should provide quantitative statistics on the formation processes of true star-planet systems at the very-low-mass end of the main-sequence; it should also nicely complement the high-angular resolution coronographic imaging survey that JWST/MIRI will carry out on these objects.

Of course, the intrinsic faintness of these objects makes it impossible to reach the same level of RV precision; this survey would rather aim at discovering massive, Neptune-like, planets orbiting L-type brown dwarfs and would allow to achieve first order statistics of their population. For instance, this program could concentrate on the ~50 brightest L brown dwarfs (with J<14 and K<12.5) and collect for each of them 25 moderate quality spectra (with typical exposure times of 30 min and S/N~40 per 2 km/s pixel) yielding RV estimates accurate to ~10 m/s and allowing one to detect >10 $M_\oplus$ planets with orbital periods <50 d (see Fig 3.4). Completing this survey would require ~75 observing nights.

3.6. RV precision : effect of telluric & OH lines

Numerous telluric lines from the Earth's atmosphere show up at nIR wavelengths, especially in the J, H & K bands (see Fig 3.8). Since they blend with stellar spectral lines and move with respect to the barycentric rest frame, they can significantly affect RV estimates if not properly taken into account, even from the very dry summit of MaunaKea (1.6 mm of H_2O on average according to Mauna Kea H_2O statistics from Gemini, supported by an independent statistical analysis from ESPaDOnS spectra).

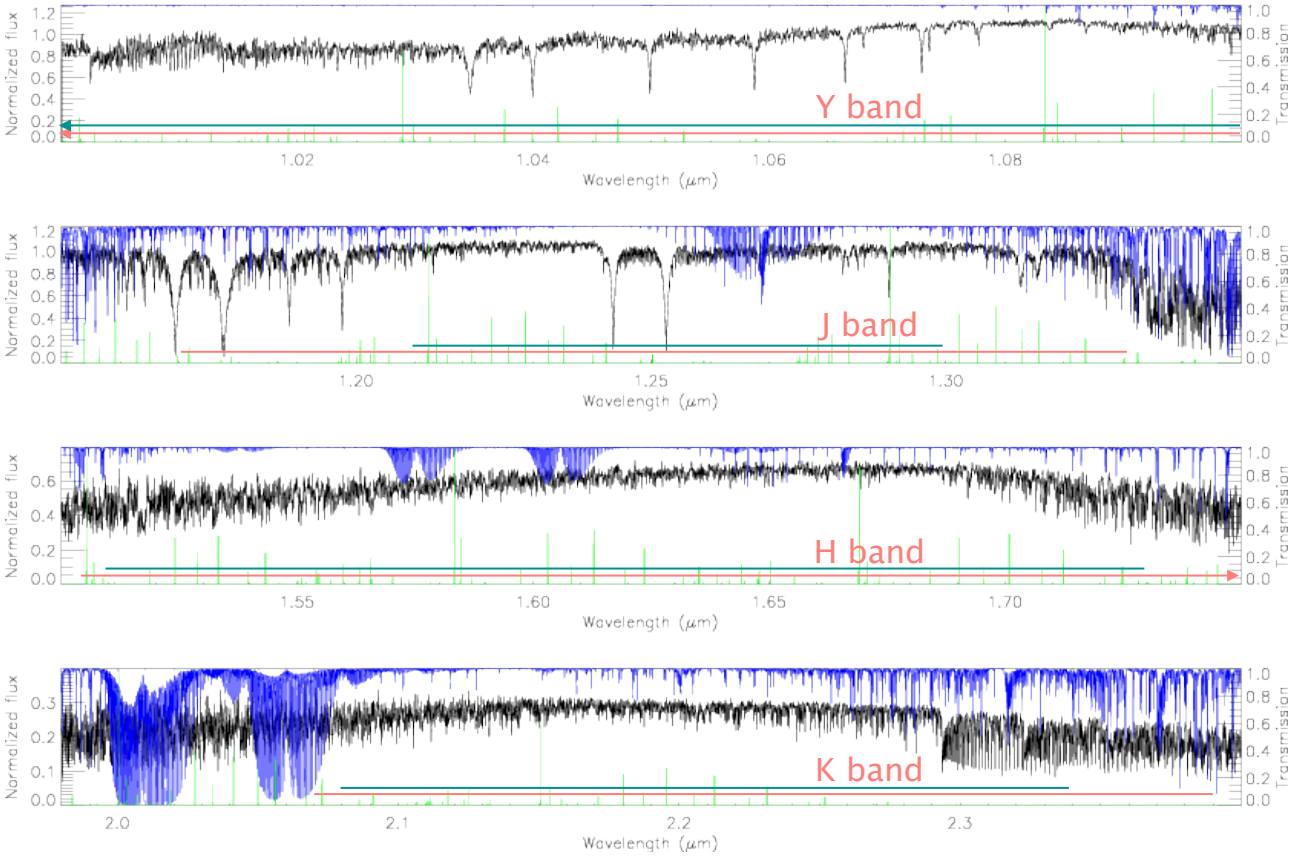

Fig 3.8: Synthetic (NextGen) spectrum of a M7 dwarf (black) along with telluric (blue) and OH (green) spectra in the Y, J, H and K bands (from top to bottom). The pink horizontal lines at the bottom of each plot depict the full band widths, while the dark green ones show the usable domains for estimating RVs (about 100%, 60%, 80% and 80% of the Y, J, H and K bands respectively, see Sec 3.6). With such spectra, the attainable RV precision can be estimated, telluric and OH lines affecting the RV budget by < 0.5 m/s in normal atmospheric conditions and using the subtraction procedure described in Sec 3.6.

The first naive method simply consists in masking out all wavelength regions showing telluric lines deeper than about 5%. An another technique consists in subtracting telluric spectrum (e.g., by using telluric standards, or models, or the sigma-clipped procedure of Bailey et al 2007, PASP 119, 228). We propose a novel approach to telluric line absorption. This approach is based on a simple physical assumption; the observed telluric absorption spectrum is the sum (in absorbance) of a finite number of chemical species that vary in relative strength. The absorbance spectrum is therefore a linear combination of individual absorbances with weight varying as a function of air mass and weather conditions (most notably for water). So, if one can build al library of these individual absorbances, then a given science observation can be calibrated using a linear combination of these absorbances. In Artigau et al (in prep) we demonstrate the efficiency of the method that we tested in the optical spectrum of HARPS. A principal component analysis (PCA) is performed to identify independently varying absorbers, and demonstrate its ability to remove 60% to 75% of the telluric lines.

Our strategy (inspired from the HARPS experience) is to mask out all regions showing H_2O lines deeper than 20% and CO_2, O_2 & CH_4 lines deeper than 50%, and to divide out the remaining lines (using either our PCA method and model of atmospheric spectra) down to a precision of better than 5% (i.e., already within reach of current correction techniques); in particular, implementing subtraction techniques allows one

to increase by ~60% the usable domain from which RVs are estimated and thus to enhance RV precision (at a given exposure time). The final usable domain spans 0.98-1.10 µm, 1.21-1.30 µm, 1.51-1.73 µm & 2.08-2.34 µm, i.e. 100%, 60%, 80% and 80% of the Y, J, H & K bands respectively (spanning themselves 0.98-1.10 µm, 1.18-1.33 µm, 1.51-1.79 µm & 2.07-2.40 µm). We plan to carry out similar subtraction techniques to remove OH lines (much more localized and thus less damaging for RVs than telluric features) from the observed spectra.

From specific simulations incorporating in particular a realistic Mauna Kea telluric spectrum, we find that telluric & OH features (when processed as described above) affect the RV budget at a level of no more than 0.5 m/s and derive that a RV precision of ~1 m/s can typically be obtained from slowly rotating mid-M dwarf spectra with a resolving power of 75,000 and a peak S/N of ~172 (per 2 km/s pixel, see Fig 8.1).

3.7. RV precision : filtering the activity jitter from Zeeman monitoring

Dark spots, bright plages or magnetic regions at the surfaces of low-mass active stars are known to generate significant distortions in spectral line profiles and therefore to produce apparent RV shifts in the collected spectra. At best, these surface features are short-lived and amount to no more than additional noise (called activity jitter) that can be averaged out on long time-scales at the cost of more measurements. However, surface features can be long-lived (especially in M dwarfs) and persist for several years, producing in some cases RV fluctuations closely resembling those caused by orbiting planets (e.g., Setiawan et al 2008, Nature 451, 38; Huelamo et al 2008, A&A 489, L9) and very difficult to average out over time.

At near-IR wavelengths, the spot/photosphere brightness contrast is significantly lower than at visible wavelengths, decreasing accordingly the amplitude of spectral line distortions caused by surface inhomogeneities and thus the associated impact on RVs. Simple simulations show for instance that the activity jitter generated by low-contrast cool spots typical to M dwarfs is ~5 times smaller in the H band than in the V band (e.g. Reiners et al 2010, ApJ 710, 432). Observations actually indicate that this damping factor is likely higher, at least a factor of ~7 (e.g. Huelamo et al 2008, A&A 489, L9) and possibly more than 10 (e.g. Martin et al, 2006, ApJ 644, L75). HARPS (V band) data show that quiet to moderately-active low-mass dwarfs exhibit typical activity jitters of 1-5 m/s (Bonfils et al 2013, A&A 549, 109), suggesting that the corresponding activity jitters in the nIR are <1 m/s and potentially even <0.5 m/s.

While the majority of early-M dwarfs are no more than weakly active and slowly rotating (with a rotation period >30 d typically), late M dwarfs behave differently with a dominant fraction exhibiting intense activity and rapid rotation - the transition between both regimes occurring at spectral type ~M4 (e.g., West et al 2008, AJ 135, 785; Reiners et al 2010, ApJ 710, 432). Activity jitters are thus expected to be potentially problematic (even in the nIR) for searches of exo-Earths orbiting very-low-mass dwarfs. A promising option consists in filtering out the activity jitter by simultaneously monitoring the large-scale magnetic field of the host star by means of spectropolarimetry (see Sec 5.1) and using empirical relationships between field topologies and activity jitters derived from standard M stars of various activity levels. Published studies on very active stars already suggest that both correlate (e.g., Morin et al 2008, MNRAS 390, 567) and a specific study is necessary to work out an analytical description of this relationship.

Results from a coordinated spectropolarimetric/RV run using NARVAL@TBL & SOPHIE@OHP in 2010 March & April (focusing on the moderately active M2 dwarf

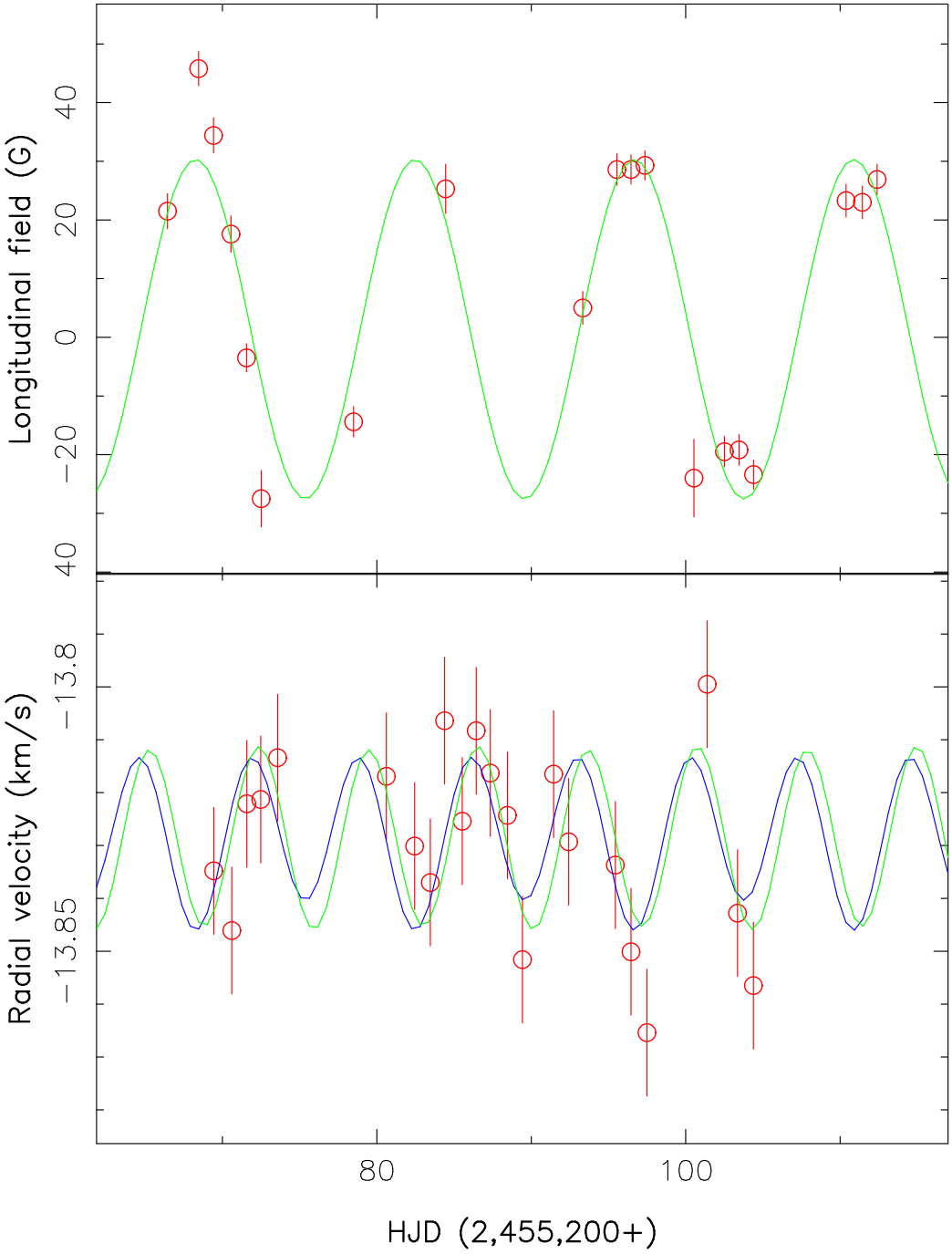

Fig 3.9: Longitudinal field (B_l, in G, top panel) & RV (in km/s, bottom panel) of the M2 dwarf DS Leo = Gl 410, as a function of heliocentric Julian date, respectively measured with NARVAL@TBL & SOPHIE@OHP in 2010 March & April (with typical error bars of 5 G & 12 m/s). The dispersion of the RV measurements about the mean is 17 m/s, i.e. about 40% larger than the typical RV error bar (12 m/s), **suggesting an RV activity jitter of ~12 m/s rms and ~35 m/s peak-to-peak**.
Fitting a periodic wave (i.e. sine+cosine+first overtones+constant) to the B_l & RV data (green curves) yields chi-square improvements of ~10 & ~2 respectively (with respect to fits with constants); in both cases, **the period yielding minimum chi-square is equal to the rotation of the star** (~14 d, Donati et al 2008, MNRAS 390, 545), **confirming that rotational modulation is detected**.
Fitting the RV data with a scaled & translated version of the longitudinal field squared (blue curve in bottom panel) yields a similar fit to the data; **the residual RV errors are ~13 m/s rms** suggesting that the remaining (unfiltered) activity jitter is at most ~5 m/s rms & 15 m/s peak-to-peak, i.e. **at least ~2.5 times smaller than the inital one**. This estimate is presently limited by the precision of our RV measurements.
More data on a sample of reference M dwarfs are needed to work out empirically what the optimal filtering process is and to obtain a more accurate estimate of its efficiency.

DS Leo = Gl 410, rotating in ~14 d, see Fig 3.9) **suggest that activity jitters can indeed be filtered out efficiently**; it also demonstrates that dwarfs with moderate activity (RV jitters of ~12 m/s rms in the optical and <2 m/s in the nIR) show clear and detectable magnetic fields from which activity filters can be derived. A more systematic investigation on a sample of reference M dwarfs is now needed for confirming that this approach is widely applicable. If validated, this procedure will provide an **on-the-fly automated correction of stellar activity jitter**. In particular, this will allow to increase the precision of RV measurements and thus the number of detectable planets; it will also enable to expand exoplanet programs to more active late-M stars that would otherwise remain out of reach.

Pulsations are another potential troublesome source of RV jitter; for a typical G dwarf, stellar oscillations can induce short term variations of up to 10 m/s on timescales of a few min (e.g. Bouchy et al 2005, A&A 440, 609) which average down to <1 m/s on exposure times longer than 20 min. In M dwarfs, pulsations are expected to have both much smaller amplitudes & shorter periods than in G dwarfs (generating negligible RV jitters for typical exposure times of 1-10 min) and should thus never become a limitation.

3.8. MC simulation of the SPIRou planet search

We conducted MC numerical simulations to realistically estimate the number of planets one can detect as a function of allocated observing time. In our simulation, realistic targets (i.e., with properties taken from the literature) are populated with planets, and observations are scheduled according to real-life open-dome statistics from CFHT. The number of visits per target is then used to derive a detection probability for all input planets, which in turns gives an estimate for the number of planets that we expect to discover by the end of the survey. We summarize here the main results of our simulations.

As an input for the MC simulations of the RV survey, we need a comprehensive list of M dwarfs with nIR magnitudes and spectral types. We compiled a list of M dwarfs from various sources, including the LSPM catalog (Lépine 2011, AJ 142, 138), the list of stars within 10 pc (mostly M dwarfs), and the spectroscopically confirmed M dwarfs in the Sloan Digital Sky Survey (SDSS, e.g., Hawley et al 2002, AJ 123, 3409). nIR photometry is taken from the 2MASS catalog, whose magnitude limit (J~16.5) is well beyond the faintest M dwarfs for which m/s RV measurements are possible on a 4m-class telescope (J~12). Stellar masses are derived from the mass-luminosity relation of Delfosse et al 2000 (A&A 364, 217), while radii are obtained from the polynomial fit of Boyajian et al 2012 (ApJ 757, 112).

Planets are assumed to show a flat logarithmic distribution in period, but a specific logarithmic distribution in mass (with 10-100 $M_\oplus$ planets being typically 22 times less abundant than 1-10 $M_\oplus$ planets). Our model only misses the relatively rare high-mass planets - but only a few are expected in the large survey we propose. There are a large number of sub-Earth-mass planets in the sample; whether these planets truly exist is still unknown and can only constrained (for orbital periods <10 d) by a survey like that we propose.

The integration is adjusted so that photon noise is 1 m/s, with an additional contribution (0.50 m/s, 1.0 m/s and 3 m/s) being added quadratically to account for the instrument RV precision. For each planet in the input catalog, one needs a detection probability derived from the number of observations and RV accuracy. We

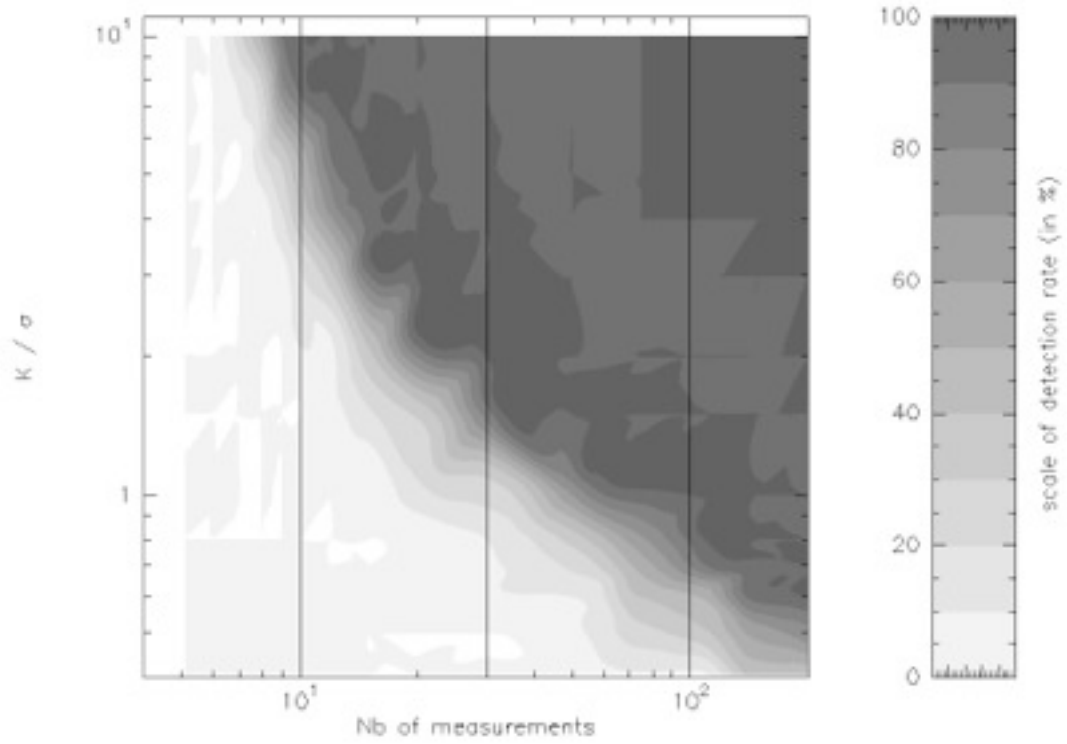

Fig 3.10: Detection probability as a function of the number of measurements and of the parameter K/σ describing planet detectability (see text). This simulation assumes planets with circular orbits.

chose to neglect the effects of eccentricity (i.e., all planets are assumed to have circular orbits) and multiplicity (i.e., a planet in a multiple system is as likely to be detected as a single one). The detectability of a planet directly depends on K/σ, where K is the semi-amplitude of the reflex motion K and σ the accuracy of the measurement. With K/σ > 10, a planet is readily detected after only a few of visits, although an accurate determination of the orbital parameters typically requires ~20 visits. With K/σ < 1, the planet RV signal is buried in the noise, and typically requires 50-70 visits to be detected at a meaningful level of significance.

To compute the detection probability of a planet we simulate a detection procedure similar to that used with HARPS/ESO. First, we generate RV data for different Keplerian orbits with N measurements at orbital phases randomly sampled across 5 consecutive orbits; noise is randomly added on each RV measurement following a Gaussian distribution of standard deviation σ. The whole RV data set for a given planet is then analyzed to find out whether the periodic signal is recovered despite the noise, using a classical period search based on floating-mean periodograms (Gilliland & Baliunas 1987, ApJ 314, 766; Zechmeister et al 2009, A&A 505, 859). The signal is considered as recovered when the FAP is below 1%. We then define the «detection probability» for a given set of observing parameters (N, K/σ) as the fraction of planets recovered with a FAP <1%. The final detection probability we obtain is shown in Fig 3.10.

4. Magnetized star/planet formation

4.1. Context

Whereas the understanding of most phases of stellar evolution made considerable progress throughout the twentieth century, stellar formation remained rather enigmatic and poorly constrained by observations until about three decades ago. One major discovery obtained at this time is that protostellar accretion discs are often associated with bipolar flows (e.g. Snell et al 1980, ApJ 239, L17), now known to be powerful, highly-collimated jets escaping the disc along its rotation axis. These jets & their collimation have been attributed to the presence of magnetic fields and to magneto-centrifugal processes (e.g. Pudritz & Norman, 1983, ApJ 274, 677). Another important discovery is that low-mass magnetic protostars are rotating significantly more slowly than predicted by a non-magnetized collapse (e.g. Bertout 1989, ARA&A 27, 351) as a likely consequence of the large-scale magnetic field coupling the protostar to its accretion disc (e.g. Königl, 1991, ApJ 370, L39). Both results demonstrate that **magnetic fields play a central role throughout stellar formation**.

The rough lines of stellar formation as we understand it now are as follows. As a result of turbulence (inherited from the diffuse interstellar medium or ISM), giant molecular clouds form clusters of dense self-gravitating condensations called prestellar cores (~0.1 pc across) in which magnetic & gravitational energies are roughly equal. The cloud starts collapsing under its own weight, with the magnetic field trying in vain to oppose the collapse (through magnetic pressure & tension). At the end of the collapse, a rotating accretion disc (hundreds to thousands of AU in size depending on the initial cloud mass) is formed within an accretion shock, usually triggering a powerful low-velocity molecular outflow. A class-0 protostar is formed at the centre of the accretion disc (at an age of a few 10 kyr since the start of the collapse), often associated with a magnetically-confined jet-like high-velocity outflow from the innermost disc regions; it eventually gives rise to an embedded class-I protostar (at an age of a few 0.1 Myr). Almost all the magnetic flux & angular momentum initially present in the dense core at the beginning of the collapse is eventually dissipated, while most of the initial cloud mass returns to the diffuse ISM; **formation is actually the phase in the life of stars where magnetic fields have the largest impact**.

Low-mass star formation is better understood than high-mass star formation[4], especially in the later stages; a few Myr after the start of the collapse, the central protostar emerges from its dust cocoon as a class-II protostar (or classical T Tauri star / cTTS) and hosts a large-scale magnetic field strong enough to disrupt the inner accretion disc and to generate a central hole (called magnetospheric gap, of ~0.2 AU across). Accretion from the inner disc rim to the surface of the protostar supposedly proceeds through discrete magnetic funnels until the disc finally dissipates at an age of ~10 Myr - with the star/disc magnetospheric interaction apparently forcing the star into slow rotation (e.g. Bouvier et al 2007, PPV). Another important role of magnetic fields throughout the cTTS phase is to control indirectly the production of high-energy photons (e.g. through coronal activity & accretion shocks); in particular, these UV & X-ray photons are responsible for ionizing the circumstellar material (thus coupling it efficiently to the field itself) and are participating in (and possibly even dominating) the heating & photo-evaporation of the disc (e.g. Ercolano et al 2009, ApJ 699, 1639;

[4] The impact of magnetic fields on high-mass star formation is also less clear and still poorly documented in the literature. As a result, we postpone to Sec 5.5 the specific description of high-mass star formation, as well as the potential contribution of high-resolution nIR spectroscopy.

Drake et al 2009, ApJL 699, L35). Before the disc finally dissipates (on a timescale of a few Myr) and the cTTS becomes a class-III protostar (or weak-line T Tauri star / wTTS), planets can be formed, with magnetic fields likely playing a significant role, e.g. on the rate at which the disc accretes & dissipates as well as on its ability at forming planets by fragmentation (e.g. Fromang 2005, A&A 441, 1); understanding the evolution of circumstellar accretion discs is thus essential to obtain plausible scenarios of planet formation.

Beyond this rough sketch, there are **many crucial questions that remain unanswered**. For instance, understanding how in practice the central protostar magnetically interacts with, accretes from, is slowed down by & eventually disperses its disc is critical if we want to obtain a more quantitative description of how stars & their planets form. Similarly, investigating the large-scale fields of wTTSs, and their differences with respect to those of cTTSs and of mature main-sequence stars, will reveal the kind of magnetospheres and winds with which Sun-like stars initiate their unleashed spin-up as they contract towards the main-sequence.

Equally important is to understand the origin of these fields, both in protostars and accretion discs: are they primordial fields from the ISM that were compressed & amplified through the cloud collapse, or rather fields produced in-situ by magneto-hydro-dynamical (MHD) processes (e.g. dynamo) after the original fossil field has been mostly dissipated? Estimating magnetic field strengths & topologies in young protostars & their accretion discs is the most direct way to address these issues and to assess quantitatively the origin & impact of magnetic fields on low-mass star & planet formation.

Finally, by looking for close-in giant planets (called hot Jupiters / hJs) around young protostars and within the inner regions of accretion discs, one can assess whether hJs are significantly more frequent around low-mass protostars than around mature stars and whether magnetospheric gaps can explain their survival around Sun-like stars. This should allow in particular to test whether hJs migrate inwards at an early evolution stage under the gravitational effect of the disc (Goldreich & Tremaine 1980, ApJ 240, 425; Alibert et al 2005 A&A 434, 343) or later on in their life through planet-planet interactions (e.g., Rasio & Ford 1996, Science 274, 954; Eggenberger et al 2004, A&A 417, 353).

4.2. Detecting magnetic fields @ nIR wavelengths

Direct magnetic measurements constraining models of star formation are difficult & rare (for a review, see e.g. Donati & Landstreet 2009, ARA&A 47, 333). For the moment, they mostly concern three stages of the formation process: the dense cores of molecular clouds, the protostellar accretion discs and the cTTSs. Given their very low temperature, dense cores can only be observed at radio wavelengths (e.g. Crutcher 1999, ApJ 520, 706); in particular, ALMA is expected to provide soon a wealth of information concerning their magnetic fields and thus to characterize how the field impacts the earliest formation stages. ALMA should also be able to detect magnetic fields & sites of planet formation in the outermost regions of close-by or very extended accretion discs.

However, magnetic fields in the inner disc regions or at protostar surfaces will be totally out of reach of ALMA and can only be investigated through nIR spectroscopy (e.g. Johns-Krull 2007, ApJ 664, 975) or optical spectropolarimetry (e.g. Donati et al 2005, Nature 438, 466; Donati et al 2007, MNRAS 380, 1297). In both cases, magnetic fields are detected through the Zeeman effect on spectral lines, and more specifically

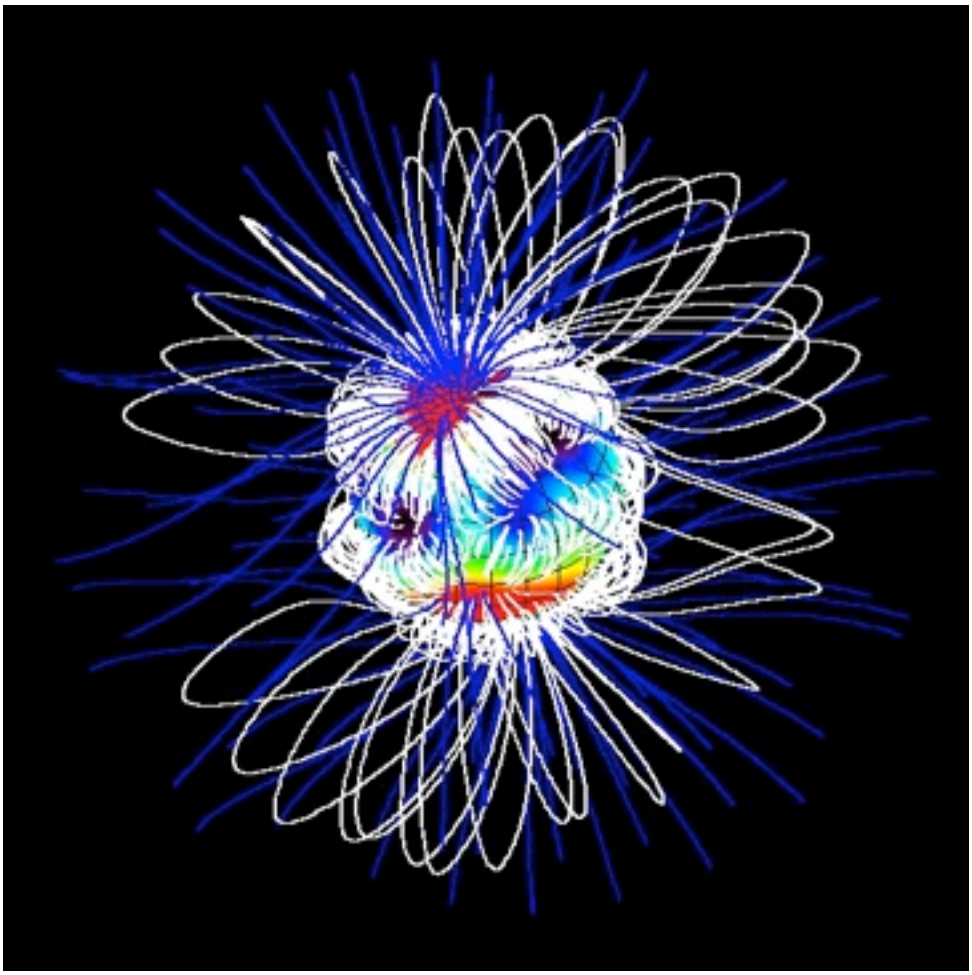

Fig 4.1: Large-scale magnetic field around the Class II protostar V2129 Oph derived from optical spectropolarimetric data secured with ESPaDOnS in the framework of MaPP (© Jardine/Donati)

through the additional broadening (with respect to non magnetically-sensitive lines of otherwise similar properties) and the polarization structures they generate within line profiles. A first exploratory survey, limited to ~15 well known cTTSs with masses > 0.3 $M_\odot$, was carried out in the framework of the MaPP (Magnetic Protostars & Planets) Large Program (LP) involving mostly the ESPaDOnS optical spectropolarimeter on CFHT (e.g. Donati et al 2011, MNRAS 412, 2454; see Fig 4.1); a second survey, concentrating on a few tens of wTTSs, is being carried out now in the framework of the new MaTYSSE (Magnetic Topologies of Young Stars & the Survival of close-in giant Exoplanets) CFHT LP.

Our knowledge of magnetic fields of protostars and their accretion discs is however still rudimentary. Up to now, only one accretion disc (FU Ori itself) has been reported as magnetic (Donati et al 2005, Nature 438, 466); moreover, field estimates are mostly available for relatively evolved objects (i.e. cTTSs or wTTSs) of masses larger than 0.3 $M_\odot$, whereas only one measurement exists for the younger, more embedded class-I protostars that are supposedly still in the process of accreting much of their mass at high rates (Johns-Krull et al 2009, ApJ 700, 1440). A much more systematic & sensitive survey of magnetic fields of all classes of protostars, including very-low-mass protostars (down to ~0.1 $M_\odot$), is thus needed.

Working at nIR wavelengths can strongly boost the sensitivity of such a survey. Class-I protostars are indeed far less obscured @ nIR wavelengths than in the

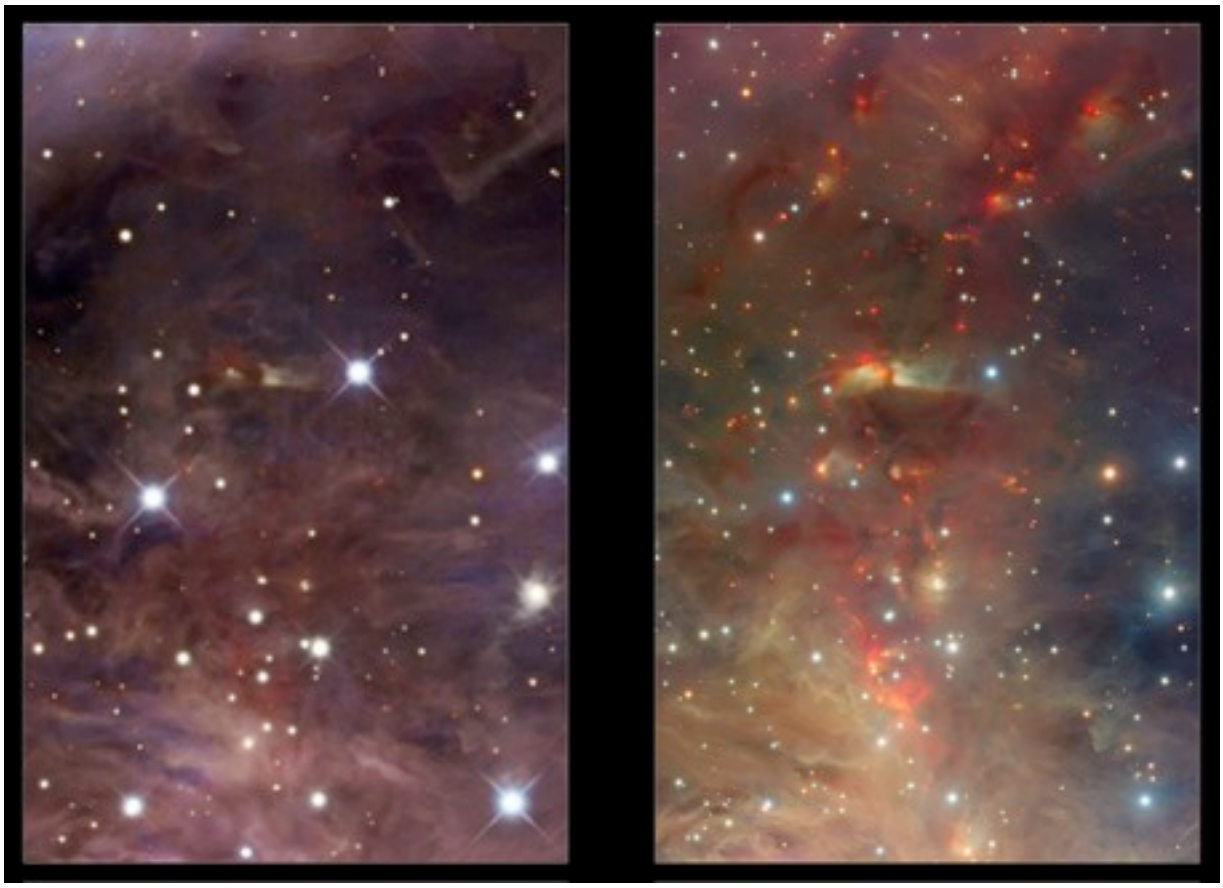

Fig 4.2: The Orion nebula as seen in visible (left) and IR (right) light (© ESO/VISTA). In the IR, dust cocoons around young stars are much more transparent

optical domain (see Fig 4.2); moreover, **the Zeeman sensitivity is also much stronger in the nIR than in the visible**, the Zeeman splitting growing linearly with wavelength with respect to the Doppler line width. Thousands of atomic spectral lines featuring a large range of magnetic sensitivities are present in the nIR, demonstrating that multiline techniques such as those used in optical spectropolarimetry (e.g. Least-Squares Deconvolution or LSD, Donati et al 1997, MNRAS 291, 658) should be straightforwardly adaptable to the nIR and very efficient at detecting & characterizing Zeeman signatures from magnetic protostars. Although still less well known than their atomic counterparts, molecular lines are both numerous in the nIR & magnetically sensitive and should also bring additional information. New methods are being developed to derive the properties of these transitions (e.g., for FeH lines of the Wing-Ford band around 1 μm, Shulyak et al 2010, A&A 523, 37) that will improve the diagnostic derived from molecular lines in the forthcoming years. With nIR spectropolarimetry, one can therefore potentially undertake a **very extensive & ambitious survey of magnetic fields in protostars & inner accretion discs**.

This survey can ideally complement **magnetic studies of prestellar cores & outer accretion discs with ALMA**[5] (which can trace fields at stages in the process of star formation earlier than those probed with SPIRou) and provide a broader context for exploring how magnetic fields impact stellar formation. In particular, coordinated observations with ALMA & SPIRou can help understanding how the fossil fields of prestellar cores link to those of protostars (see Sec 4.3); they can also provide a view of magnetic fields & planet formation within accretion discs across a wider range of radii (see Secs 4.4 & 4.5).

4.3. Magnetic fields of protostars & magnetospheric accretion models

By detecting Zeeman signatures in photospheric absorption and accretion-powered emission lines of young low-mass protostars and by monitoring them as the stars rotate, we can model their large-scale magnetic topologies (e.g. Donati et al 2011, MNRAS 412, 2454; see also Fig 4.1). From this, we can quantitatively address, for a statistically significant sample of class-I, -II & -III protostars, several key issues concerning the structure & fate of newly born stars, and in particular points such as (i) what is the origin of their magnetic fields (e.g. fossil or dynamo), (ii) how do these magnetic fields connect the protostars to their accretion discs, (iii) how do these fields control accretion from the discs and how can they slow down the rotation of the protostars, (iv) how do they participate (along with accretion disc fields) in launching collimated jets, (v) how importantly do they contribute to the photo-evaporation of the disk through the coronal X-rays they indirectly produce, (vi) to what extent do magnetism and magnetospheric accretion modify the internal structure of protostars, and (vii) with which magnetic topologies do protostars start their unleashed spin-up towards the main sequence once they dissipated their accretion discs?

Results from MaPP already suggest that **fields of cTTSs are generated by dynamo processes** given their overall similarity with those of low-mass main sequence stars - and in particular the sharp transition in large-scale field properties between fully-convective & non-fully-convective stars (Donati & Landstreet 2009, ARA&A 47, 333; Gregory et al 2012, ApJ 755, 97); this conclusion is further supported by the discovery that large-scale fields of cTTSs are often variable on timescales of a few yrs, demonstrating that they are generated by non-stationary dynamo processes (e.g. Donati et al 2011, MNRAS 412, 2454). These results also suggest that **the rotation periods of cTTSs correlates well with the intensities of their large-scale fields**, slower rotation being observed in stars with stronger magnetic dipolar components (for a given mass accretion rate) - providing independent support for the idea that star-disc magnetic coupling is capable of

[5] More precisely, ALMA will be capable of using all the techniques currently available in the sub-mm & far-IR for the study of star-forming regions and protostellar discs. For example, circular polarization measurements will allow for measuring the strength of the line-of-sight component of the magnetic fields using appropriate Zeeman-sensitive molecules (e.g. CN & CCH; Crutcher et al 1999, 514, L121), while linear polarization measurements on other abundant molecules (e.g. CO & CS) will trace the orientation of the magnetic field in the plane of the sky at different densities through the so-called Goldreich-Kylafis effect (Golreich & Kylafis 1981, ApJ 243, L75; Cortes et al 2005, ApJ 628, 780). Linear polarization studies of dust emission, also available to ALMA, have been extensively used for many years for the same purpose (Hildebrand et al 2000, PASP 112, 1215), and the so-called Chandrasekhar-Fermi technique (Chandrasekhar & Fermi 1953, ApJ 118, 113) can be applied to such measurements to provide an indirect determination of the strength of the plane of the sky component of the magnetic field, therefore potentially complementing Zeeman measurements. Finally, line width comparisons of coexistent ion & neutral molecular species (e.g. HCO^+ & HCN) observable at several transitions will allow a further characterization of magnetized turbulence through the measurement of important quantities such as the turbulent ambipolar diffusion length scale, which in turn allows for another independent measure of the plane of the sky magnetic field strength (Li & Houde 2008, ApJ 677, 1151; Falceta-Gonçalves et al 2010, ApJ 713, 1376; Hezareh et al 2010, ApJ 720, 603).

regulating the angular momentum of protostars. However, deriving a thorough description of how large-scale fields of protostars depend on parameters such as mass & age requires collecting data on a much more extended sample than the current one (of ~15 cTTSs), and that includes in particular both class-I and class-III protostars.

More specifically, a typical goal would be **to monitor regularly about 50 class-I and 200 class-II & -III protostars** featuring a wide range of parameters (e.g. masses, ages, rotation periods, mass accretion/ejection properties) and selected in different stellar formation regions (e.g. Taurus/Auriga, ρ Oph, TW Hya Association, Lupus, ONC - with typically 10 class-I and 40 class-II & -III well-selected protostars per formation region) in order to ultimately investigate how magnetic properties correlate with fundamental parameters. The improved sensitivity brought by nIR observations allows one in particular to recover not only large-scale surface magnetic fluxes (derived from phase-resolved sets of polarized line profiles) but also the relative amount of unresolved small-scale magnetic fields packed in close bipolar groups (e.g. by comparing field fluxes obtained from polarized Zeeman signatures with field strengths derived from Zeeman broadening of unpolarized spectral lines).

With such data, quantitative studies of how protostars accrete material from their accretion discs and how this process impacts their structure & rotation evolution can be carried out for the first time and **the corresponding models can be directly confronted to observations**. One can for instance retrieve the location & geometry of accretion funnels (e.g. Gregory et al 2008, MNRAS 389, 1839; Romanova et al 2011, MNRAS 411, 915), investigate how the resulting accretion shock affects the atmosphere of the star (e.g. Orlando et al 2010, A&A 510, 71) and evaluate the impact of accretion on structure (Baraffe et al 2009, ApJ 702, L27) & angular momentum content (e.g. Zanni & Ferreira 2013, A&A 550, 99; see also Matt & Pudritz 2008, ApJ 681, 391) of the newly born star. In particular, class-I protostars should be well suited for investigating magnetospheric accretion at higher accretion-rate regimes.

For such observations, one needs (i) **high spectral resolution, typically 75,000,** (ii) reasonably **high S/N ratios - typically 100** (in the JHK bands, per 2 km/s pixel), and of course (iii) **access to polarization information in line profiles** (especially circular polarization) to detect Zeeman signatures probing magnetic fields with enough precision on their strengths & shapes. Obviously, one needs to collect as wide a spectral domain as possible in a single exposure (typically 0.98-2.35 μm, i.e. the YJHK bands) in order to (i) maximize the number of photospheric lines from which Zeeman signatures are extracted and improve the precision to which magnetic fields are detected & modeled, (ii) record as many different spectral proxies as possible (e.g. lines formed at the footpoints of accretion funnels, or at the inner rim of the accretion disc) to monitor magnetospheric accretion processes simultaneously with (and further constrain) the magnetic topology. Weak levels of polarization crosstalk (typically <1%) & linear polarization filters (e.g. rotating half-wave retarders) are also welcome (e.g. for detecting weak circular polarization signatures in emission lines exhibiting strong linear polarization).

Thousands of magnetically sensitive & insensitive photospheric lines are available for stellar magnetometry, both from atoms & molecules. Around 2.22 μm for instance, 3 Ti I lines @ 2.221, 2.223 & 2.227 μm (w/ respective Landé factors of 2.08, 1.66 and 1.58), 1 Sc I line @ 2.226 nm (w/ Landé factor of 0.50), as well as the magnetically insensitive CO overtone lines around 2.3 μm are regularly used to estimate magnetic field strengths in protostars (e.g. Johns-Krull 2007, ApJ 664, 975; Johns-Krull et al 2009, ApJ 700, 1440). Obviously, **lines in the K band are most interesting** given the increased Zeeman splitting resulting from the longer wavelength. Concerning

accretion proxies, Paβ, Paγ & Brγ (located at 1.28, 1.09 & 2.17 μm respectively) are known to be reliable tracers of accretion, showing in particular minimal contamination by outflows as opposed to Hα (e.g. Kurosawa et al 2005, MNRAS 358, 671). The 1.083 μm He I line offers at the same time a promising diagnostic to probe the magnetically controlled star-disc interaction & wind-launching region in accreting young stars (Edwards et al 2006, ApJ 646, 319).

Being partially obscured by their dust cocoon, class-I protostars are rather faint but ~10 of them with K<11 can be found in each nearby star forming regions With an average K magnitude of ~11 and a total exposure time of about 1 hr per star & per visit (yielding S/N~110 per 2 km/s pixel, see Sec 8.5), monitoring ~50 class-I protostars @ 20 rotation phases (to be able to disentangle rotational modulation from intrinsic variability - usually very significant in protostars) requires a total observing time of ~125 nights. Given how embedded and reddened class-I protostars are (see Fig 4.3), more than 90% of their 0.98-2.35μm spectral content concentrates into the K band; lacking a K-band access thus implies losing the opportunity of observing this sample and of carrying out the corresponding science, despite being foreseen as the newest and most original potential contribution of SPIRou in this field.

Regarding class-II & -III protostars in close-by stellar formation regions (e.g. Taurus & ρ Oph, see Fig 4.3), a large fraction of them have JHK magnitudes in the range 7-12. Monitoring a sample of 200 of them (~40 per selected star forming region) with an average K magnitude of ~9.5, again at 20 rotation phases, will require an additional ~125 nights.

The overall survey on magnetized star / planet formation that we propose to carry out with SPIRou therefore requires a grand total of ~250 observing nights. In a discovery phase of 125 observing nights, we will concentrate mostly on the brightest class-I-III protostars located in Taurus/Auriga, ρ Oph, and TWA, leaving the other 2 star forming regions for a subsequent observing phase.

Given the spectral content of the 0.98-2.35μm domain on the one hand, and given how the Zeeman effect increases with wavelength on the other hand, we find that the K band alone concentrates ~70% of the spectropolarimetric information, implying that an instrument with the K band will be typically 3x more efficient than the same instrument w/o K - clearly demonstrating the crucial importance of this band.

Our program will nicely complement observations of class-0 protostars with ALMA at various stages of evolution and for different masses; in particular, it may reveal how the dynamo fields of class-II & -III protostars relate to the fossil fields of class-0 protostars - a yet unclear piece of the stellar formation puzzle. The final target selection will be carried out as part of the SPIRou science preparation (with the construction of a SPIRou Input Catalog), and will be exploiting the latest results from Spitzer & Herschell on nearby star forming regions to ensure that the best possible targets are selected.

4.4. Magnetic fields of gaseous inner accretion discs

The physics of protostellar accretion discs is still poorly constrained by observations. In particular, gas (rather than dust) densities & temperatures of inner accretion discs are difficult to pin down and are thus uncertain - yet very important as gas vastly dominates the mass of protostellar accretion discs. For instance, measuring how gas densities in accretion discs decrease with time is crucial for deriving reliable estimates of typical disc lifetimes for different protostellar masses. In the last decade,

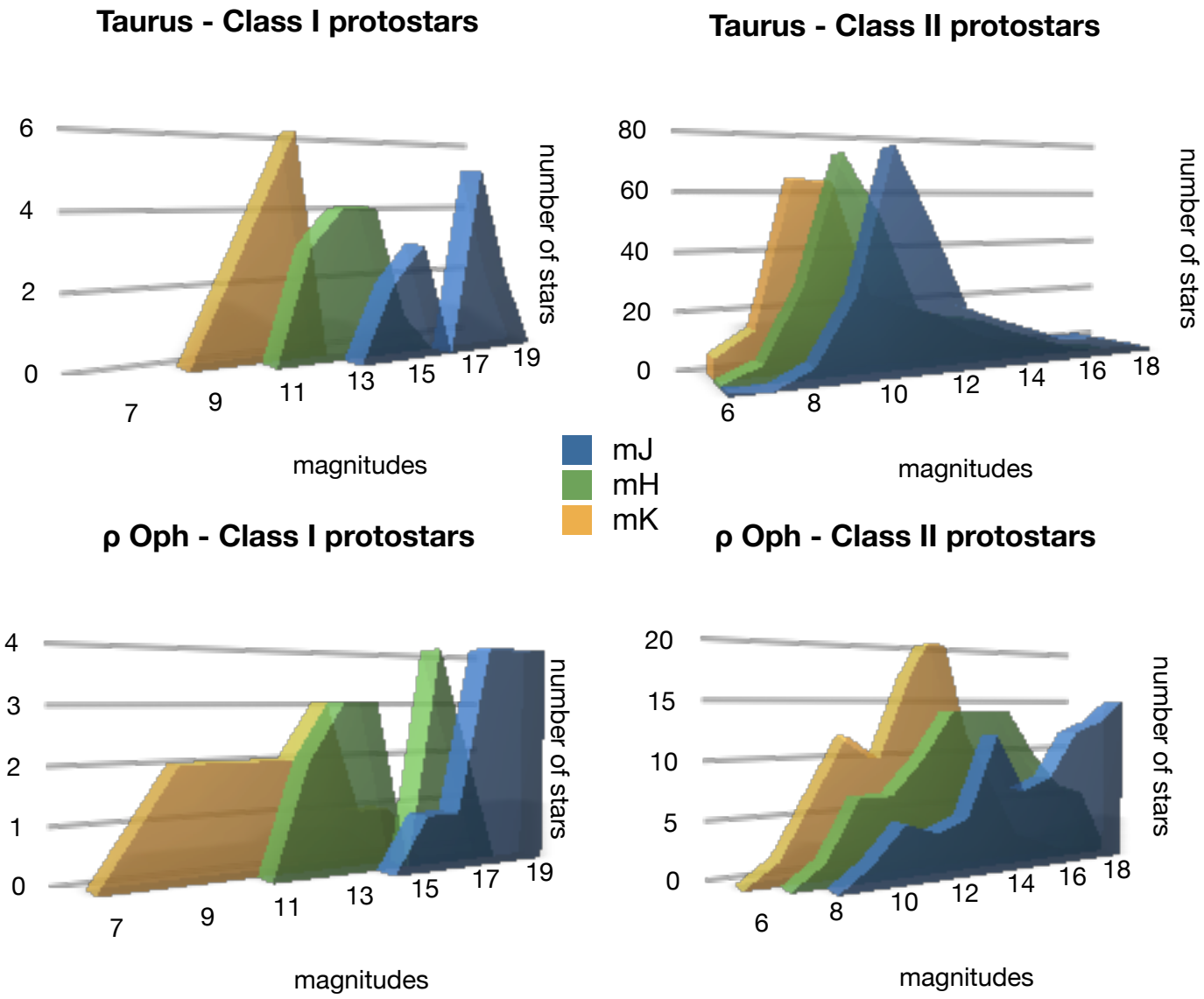

Fig 4.3: JHK magnitude histograms of Class I (left) & II (right) protostars in Taurus (up) and ρ Oph (bottom). Class I protostars are mostly brighter than 12 in K only (as a result of obscuration, especially in ρ Oph), whereas a significant fraction of Class II protostars are accessible in all 3 bands.

progress has been made in developing both observational probes of gaseous inner discs as well as the theoretical models needed to start interpreting the observations (Najita et al 2007, PPV review).

Although often neglected in models, magnetic fields within protostellar discs can severely affect the gas and are thus likely **a crucial ingredient of stellar formation** – magnetic fields are indeed presumably responsible for the enhanced viscosity and hence accretion rates in protostellar accretion discs via MHD instabilities such as the Magneto-Rotational Instability (MRI, e.g., Balbus 2003, ARA&A 41, 555). However, the origin of disc fields and their impact on the physics of accretion discs on the one hand, and on the star/disc interaction on the other hand, are still mostly speculative, especially in inner disc regions where these fields are expected to have the largest effect.

Magnetic fields are also predicted **to drastically reduce the size of accretion discs** produced during the cloud collapse as a result of magnetic braking (Shu et al

1987, ARA&A 25, 23; Basu & Mouschovias 1995, ApJ 452, 386; Machida et al 2005, MNRAS 352, 369; Banerjee & Pudritz 2006, ApJ 641, 949; Hennebelle & Fromang 2008, A&A 477, 9), from hundreds of AUs in purely hydro-dynamical cases down to a tens of AUs when fields typical to protostellar cores are taken into account. This is in apparent contradiction with observations demonstrating that class-I and -II protostars are in most cases surrounded by extended accretion discs (e.g. Watson et al, 2007, PPV). Although simulations show that fields tilted to the clouds rotation axes (e.g. Hennebelle & Ciardi 2009, A&A 506, L29) or non-ideal MHD (e.g., Machida et al 2011, PASJ 63, 555) can reduce the discrepancy with observations, it is nonetheless quite clear that magnetic fields can strongly impact the extent & overall structure of accretion discs and more observational & theoretical studies are needed to investigate the issue at a deeper level.

Whereas models of magnetized cloud collapse usually assume that disc magnetic fields are primordial (e.g. Banerjee & Pudritz 2006, ApJ 641, 949; Hennebelle & Fromang 2008, A&A 477, 9), other models propose that they could also be produced through dynamo processes (e.g. Brandenburg 2005, ApJ 625, 539) - with both models predicting different field topologies (mostly poloidal & toroidal fields respectively). The field strength within the disc is also a matter of speculation, with non-ideal MHD simulations of magnetized cloud collapse predicting magnetic fluxes to be strongly dissipated in the so-called dead zones where ionization is low (e.g. as a result of high disc densities, Machida et al 2007, 670, 1198; Shu et al 2007, ApJ 665, 535). Magnetic fields in the inner disc are also thought to participate actively in star-disc interactions and in jet-launching, though the exact mechanism of these phenomena is not yet clear (e.g. Shu et al 1994, ApJ 429, 781; Ferreira et al 2006, A&A 453, 785).

The protostellar discs most directly accessible to observations and first studied in some detail are FUOrs (of which FU Ori is the prototype). FUOrs are thought to be fairly young protostellar objects undergoing so strong an accretion outburst that the central star is mostly outshone by the disc (e.g. Hartmann & Kenyon 1996, ARA&A 34, 207). The only existing direct measurement of magnetic fields in the central regions of an accretion disc (obtained via optical spectropolarimetry) concerns FU Ori itself - a 0.1 Myr accretion disc surrounding a low-mass protostar. At a radial distance of 0.05 AU from the centre, the disc is found to host a magnetic field mostly perpendicular to the disc plane, reaching a strength of ~1 kG and concentrating in the ~20% of the disc plasma that rotates at strongly sub-Keplerian velocities (Donati et al 2005, Nature 438, 466). This result indicates that the origin of the field is probably fossil (rather than dynamo generated) and that the field survived magnetic dissipation at disc densities much higher than initially predicted, suggesting that yet unidentified ionization mechanisms may operate within accretion discs and hence limit the extent of dead zones (e.g. Donati & Landstreet 2009, ARA&A 47, 333; Combet et al 2010, A&A 519, 108).

Estimating the gaseous content in the inner regions of different types of accretion discs (including non-outburst ones), **investigating** (whenever possible) **their magnetic field strengths & topologies** (e.g., with respect to that of FU Ori) and looking for potential correlations between the disc & field properties (to find out whether & how fields can impact discs) requires carrying out a survey in a statistically significant sample of discs of various evolutionary stages. Applying tomographic techniques similar to those used to map accretion discs of cataclysmic variables (e.g. Marsh & Horne 1990, ApJ 349, 593; Steeghs et al 1997, MNRAS 290, L28; see Fig 4.4) can for instance provide observational constraints on how absorption/emission (and therefore densities & temperatures) vary with radius within inner regions of

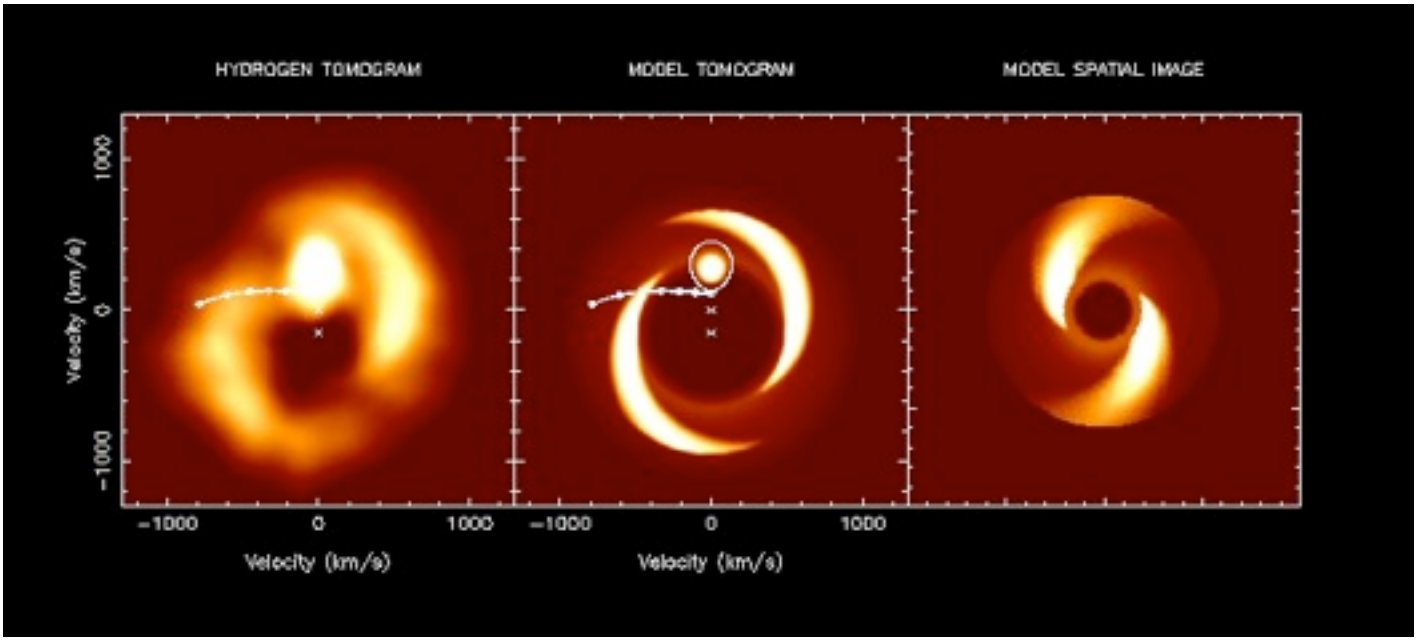

Fig 4.4: Doppler tomography of line emission in accretion discs of cataclysmic variables. A similar technique can be used to retrieve radial distributions of line emission within protostellar discs (© D Steeghs).

protostellar discs and how typical disc densities evolve from Class I to transitional discs.

In this respect, **nIR** (and especially K-band) **spectroscopy & spectropolarimetry** at a resolving power of ~75,000 is particularly well suited, giving access to many magnetically-sensitive atomic absorption lines (for FUOrs) and to several molecular emission features like the H_2 emission line (@ 2.12 nm), the (magnetically insensitive) CO overtone emission lines (@ 2.3 μm) and the hot H_2O emission lines, all presumably probing the discs of young low-mass and high-mass stars (e.g. Bary et al 2008, ApJ 678, 1088). Measuring density distributions within discs & estimating disc lifetimes typically require collecting spectra of protostars with S/N~100 per 2 km/s pixel, implying that many class-I & -II objects in nearby star forming regions are accessible (mostly in the K band for class-I objects, see Sec 4.3 & Fig 4.3). Extrapolating from results of FU Ori, magnetic detections require spectra with much higher S/N ratios, typically ~500 per 2 km/s pixels. K magnitudes of known FUOrs (~20 objects) are in the range 7-8, allowing the requested S/N ratios to be achieved in the K band for exposure times of ~1 hr; discs from most class-II protostars in close-by star forming regions are also potentially accessible.

Observing a typical sample of ~10 discs (i.e. a significant fraction of the accessible sample, including in particular several FUOrs) of various properties (e.g. with host stars of different masses and different evolutionary stages, with different accretion rates, with & without jets) with one visit per night for ~40 consecutive nights (to monitor Keplerian periods from the inner disc rim out to ~0.5 AU) will require a total of **~50 nights**.

Such observations could in particular nicely complement simultaneous ALMA observations revealing the properties (including magnetic field) in the outer disc regions (typically beyond 1 AU). More specifically, continuum & CO ALMA observations could be used to detect 1.3 mm flux around protostars at the cTTS stage and beyond (up to zero-age-main-sequence) in order to characterize the gas disc, i.e. estimate its extent, mass, temperature and CO depletion; this would allow in particular to follow

the dissipation processes driving the evolution of protostellar discs ranging in mass from 0.5 to 3 $M_{\odot}$.

4.5. Planet formation & the survival of hot Jupiters

Arguably the biggest surprise from the discovery of exoplanets is that so many are in orbits very untypical of the solar system, with in particular Jupiter-mass planets very close to their host star (hot Jupiters / hJs). It has not been possible to think of scenarios in which they could have formed there, so the current thought is that they migrated from farther out, in ways that are, as yet, poorly understood (e.g. as a result of gravitational interactions from either the disc or other massive planets/ companions). The recent discovery that orbital axes of exoplanets can be frequently misaligned with the rotation axes of their host stars (e.g. Hébrard 2008, A&A 488, 763; Triaud et al 2010, A&A 524, 25) suggests that migration may also be due to dynamical interactions with a third body through the Kozai effect (Winn et al 2010, ApJ 718, L145); magnetic stars interacting with their disks could potentially produce similar misalignments (Lai et al 2011, MNRAS 412, 2790). In this context, detecting hJs around protostars and deriving reliable estimates of disc lifetimes & distributions of gas densities at various formation stages are of prime importance for pinning down timescales on which giant planet form & migrate inwards, and for working out how these migrating bodies successfully avoid falling into their host stars.

Magnetic fields in discs are potentially important since fields are expected to impact significantly the formation, disc-induced migration & orbital inclination of protoplanets. More specifically, discs fields & associated MHD turbulence can potentially inhibit fragmentation through gravitational instabilities (e.g. Hennebelle & Teyssier 2008, A&A 477, 25) and modify the subsequent formation of giant planets (e.g. Fromang 2005, A&A 441, 1). Fields can also slowdown or even stop the migration of protoplanets (e.g. Terquem 2003, MNRAS 341, 1157) and possibly modify the rate at which they accrete mass from the disc (e.g. Machida et al 2006, ApJ 649, L129); they can even lead to the production of outflows from giant planets, similar to those detected in young stars. By disrupting the inner regions of accretion discs and creating central magnetospheric gaps as well as by generating strong winds, magnetic fields of class-I and -II protostars can also indirectly stop the inward disc-induced migration of giant planets formed earlier in the outer disc (e.g. Lin et al 1996, Nature 380, 606; Romanova & Lovelace 2006, ApJ 645, L73; Lovelace et al 2008, MNRAS 389, 1233; Vidotto et al 2009, ApJ 703, 1734); this would make them end their migration at orbital distances of ~0.05 AU (typical to hJs and compatible with observed magnetospheric gaps of cTTSs) and would help them survive, avoiding them to fall into their host star. Various observational experiments can be devised to quantitatively test these ideas and to **constrain models of giant planet formation & migration**.

Using the protostar survey described in Sec 4.3, one can can look for periodic RV changes of TTSs that may reveal the presence of hJs (producing typical peak-to-peak RV amplitudes of 0.1-1 km/s on periods of a few days). Though non-trivial given the high level of activity of TTSs (generating RV jitters at visible wavelengths comparable to or larger than the RV reflex motion of potential hJs), detecting hJs is nevertheless possible. As mentioned in Sec 3.8, RV jitters are expected to be 5-10 times smaller at nIR wavelengths than in the visible; moreover, by accurately modeling the activity of wTTSs with advanced imaging methods, one can **filter most of the activity-induced RV changes down to a level** (~30 m/s) **at which hJs should become detectable**.

The predicted number of hJs orbiting TTSs is unclear as of today. Since slightly less than 1% of mature Solar-like stars host hJs, one can expect that TTSs should also host hJs with at least the same frequency if these hJs are generated through disc migration; alternatively, hJs will be far less numerous around TTSs if hJs are formed through planet-planet interaction / scattering. If the fraction of hJs around TTSs is ~1%, we expect to find ~2 of them in our sample of ~200. Our observations should then **bring the first observational confirmation of whether disc migration is indeed the main mechanism for generating hJs, or whether planet-planet interaction / scattering is to be preferred.** Obviously, this result would represent a major observational achievement and would be a significant step forward in our understanding of hJs. Note that, to achieve this goal, we will make a simultaneous use of both velocimetric & spectropolarimetric capabilities of SPIRou.

Another option would be to look for potential gaps in the radial distribution of disc gas densities derived from time resolved series of nIR disc lines (using disc tomography, see Sec 4.4 & Fig 4.4) that could reveal the presence of migrating giant planets (e.g. Clarke & Armitage 2003, MNRAS 345, 691; Powell et al 2012, MNRAS 426, 3315). Provided disc magnetic fields are also detected, looking into whether density gaps in discs radially coincide with maxima in magnetic flux distributions can potentially demonstrate the role of magnetic fields in planet migration. Forming exo-protoplanets can be detected as well through their outflows (using nIR spectral proxies specific to winds and jets) and even mapped within the accretion disc thanks to Doppler tomography. Such experiments typically require spectra with S/N~100 per 2 km/s pixel with dense sampling of Keplerian periods within the inner disc regions.

Coordinated observations with ALMA could also reveal **giant planets embedded in the outer regions of protostellar accretion discs** as well as the potential gaps, spiral waves and circumplanetary discs that are presumably associated with such protoplanets. ALMA observations are likely to be mostly targeting protoplanetary discs viewed nearly face-on from the Earth, to maximize the spatial resolution achievable in the disc, i.e. about 2 AU at a distance of 140 pc. Although RV measurements (capturing only the velocity along the line-of-sight) are obviously less sensitive to such geometries, they should nevertheless provide enough precision for detecting at least close-in giant exoplanets orbiting in the inner-disc magnetospheric gap; alternately, ALMA observations can also yield valuable (though slightly less resolved) information on the outer regions of discs viewed at intermediate inclinations.

Spectra with S/N~100 per 2 km/s pixel & dense sampling of several successive rotation cycles (to disentangle properly rotational modulation from intrinsic variability) are required for this program, which can therefore be carried out on most protostars / accretion discs of close-by star-formation regions. **The corresponding sample thus fully overlaps with those of Secs 4.3 & 4.4**.

5. More stellar physics: from dynamos, starspots & weather patterns to the formation of brown dwarfs & massive stars

In addition to the two main science goals described above (in Secs 3 & 4), SPIRou can tackle a large number of other first-rate programs, some of them focussed again on red & brown dwarfs - but aiming this time at unveiling some of their still-enigmatic physics (rather than at detecting their potential planets). Studying the properties of starspots on active stars and of circumstellar environments, or investigating the formation of massive stars are other promising options.

5.1. Dynamo processes in red & brown dwarfs

In the last 20 years, red & brown dwarfs have triggered an increasing amount of interest. Due to their intrinsic faintness, little was known about these objects before - and despite considerable progress in recent years, their physics, internal structure & atmospheric properties are still subject to discussions, with a number of key issues (e.g. atmospheric chemistry, dynamo processes) remaining largely speculative. For instance, quantities as fundamental as the emergent spectrum and even the radius are still controversial and often in disagreement with predictions. For instance, synthetic spectra of low-mass & very-low-mass dwarfs in the nIR are significantly off (lacking in particular a number of molecular and even atomic species, e.g. Reiners et al 2007, A&A 473, 245; Rice et al 2010, ApJS 186, 63), thereby suggesting that atmospheric modeling (very complex in ultra cool dwarfs) is still work in progress. Radii of active red dwarfs, observed to be significantly larger than those of non-active dwarfs (of otherwise similar spectral types, e.g. Morales et al 2008, A&A 478, 507), provides another striking example of these critical modeling puzzles for which no obvious solution is foreseen.

Understanding dynamo processes in fully-convective bodies to the point of correctly predicting large-scale magnetic topologies of mid-M to early-L dwarfs has also been a long-lived issue and a theoretician nightmare. Whereas early studies initially suggested that fully-convective dynamos were mostly operating on small scales, newer models & recent numerical simulations gradually showed that large-scale fields are also likely to be triggered; the exact topology of these fields (e.g. the relative strengths of the poloidal & toroidal fields, as well as the degree of axisymmetry of the poloidal component) is however still unclear and predictions significantly differ from one model to another (e.g. Dobler et al 2006, A&A ApJ 638, 336; Browning 2008, ApJ 676, 1262). In simulated convective cores of massive stars (Brun et al 2005, ApJ 629, 461, see Fig 5.1), recent results have shown that super-equipartition dynamo states can exist, in which the magnetic energy built by dynamo action can be up to 10-times larger than the kinetic energy of the convection itself (Featherstone et al 2009, ApJ 705, 1000). Although not directly applicable to M dwarfs already, this result nonetheless illustrates that important discoveries are yet to come in this research field.

Although intense magnetic fields had been reported (about 25 years ago) to be present at the surfaces of fully-convective dwarfs, no clues existed about their large-scale strengths & topologies. Only recently, spectropolarimetric data (collected with ESPaDOnS@CFHT) revealed that active mid-M dwarfs are capable of hosting strong mostly-axisymmetric poloidal fields with no apparent need for differential rotation (e.g. Donati et al 2006, Science 311, 633); radio observations independently

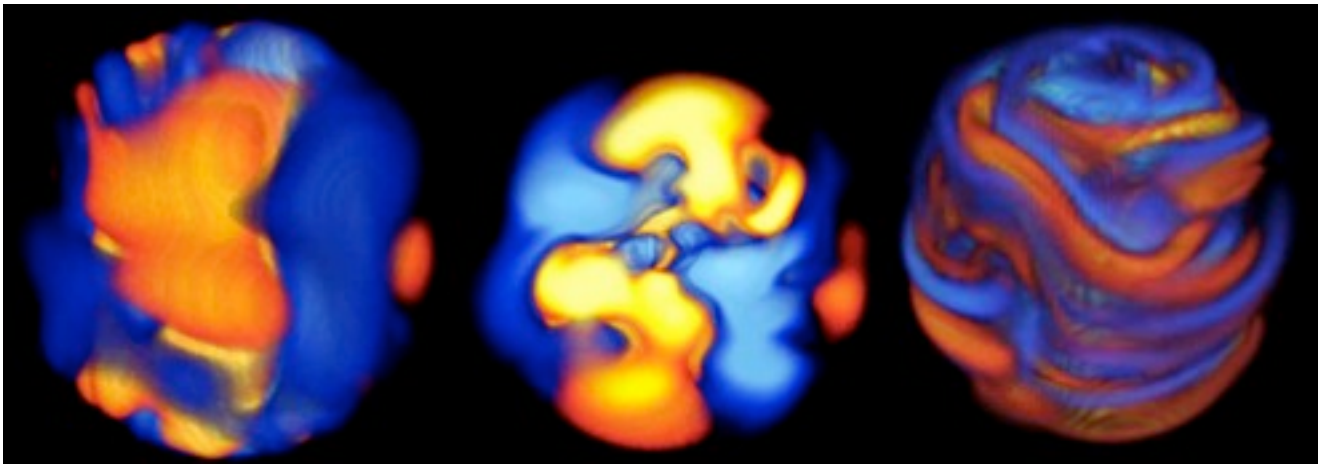

Fig 5.1: 3D MHD simulations of dynamo processes in convective cores of massive stars (left & middle: convective velocity field & equatorial slice, right: toroidal magnetic field) suggest that large-scale ribbon-like field structures can form persistent magnetic wreaths around the star (© S Brun)

confirmed that strong large-scale fields are indeed present in some red & brown dwarfs up to spectral types of at least L3 (e.g. Berger, 2006, ApJ 648, 629). More specifically, a first magnetic survey of active M dwarfs unambiguously established that **fields drastically change across the full-convection boundary**, getting stronger, simpler & almost purely poloidal & axisymmetric at spectral types later than M3 (e.g. Morin et al 2008, MNRAS 390, 567). The latest results suggest that the situation becomes more complex in late-M dwarfs with dynamo action exhibiting an apparent bi-stable behavior, i.e. capable of generating either intense or weak large-scale fields at given masses & rotation rates (Morin et al 2010, MNRAS 407, 2269 & 2011, MNRAS 418, L133). The potential relationship between this bi-stable behavior and the putative existence of super-equipartition dynamo regimes is promising and certainly worth exploring.

Obviously, time is ripe for a new, more ambitious & systematic exploration of the magnetic properties of M & early L dwarfs - both at small & large scales - to guide modern models & numerical simulations of fully-convective dynamos towards a more global & successful description of magnetic field generation in low-mass stars, as well as to understand better the impact of dynamo fields on stellar structures & atmospheres (e.g. Chabrier et al 2007, A&A 472, L17). For this new survey, **nIR spectropolarimetry is the obvious & optimal choice:** in addition to coinciding with the spectral window where late-M & early-L dwarfs radiate most of their photons, the nIR domain enables one to yield simultaneously accurate estimates of both small- & large-scale fields (using unpolarized & circularly polarized line profiles, respectively) given the enhanced Zeeman splitting at longer wavelengths.

For this survey, we definitely need high spectral resolution (typically 75,000 or 4 km/s) to provide as much detail as possible on the shape of spectral lines & Zeeman signatures; this is especially important for low-mass dwarfs whose intrinsically small radii strongly reduce the amount of rotational broadening in spectral lines. Performing reliable & achromatic circular polarimetry of spectral lines is obviously important here; we also need the largest possible spectral domain accessible in a single exposure (i.e. 0.98-2.35 μm, the YJHK bands) to ensure that we maximize the number of atomic & molecular lines from which Zeeman signatures are extracted and improve the precision to which magnetic fields are detected & modeled (as for studies of magnetic protostars, see Sec 4.3).

Typically, S/N~100 per 2 km/s pixel is required for this program, corresponding to a limiting K magnitude of ~11 for exposure times of ~1 hr (see Sec 8.5); this implies that hundreds of M dwarfs are accessible while a dozen of the brightest early-L dwarfs should be within reach (see Sec 3). Monitoring ~100 M dwarfs (e.g. from the late-M volume-limited sample up to 20 pc of Reiners & Basri 2010, ApJ, 710, 924) at ~10 rotation phases would require **a total amount of observing time of ~125 nights**. Note that this study can easily be coupled to the exoplanet search described above (see Sec 3) if spectropolarimetry is achieved at all times since both programs should overlap on a large fraction of their samples (the non-overlapping part corresponding to ~50 nights).

5.2. Weather patterns on brown dwarfs

Following the discovery of ultra-cool L & T brown dwarfs (BDs), huge efforts have been invested to model their atmospheres, with only limited success up to now. First among unanswered questions is the fact that early-T dwarfs tend to have absolute J magnitudes brighter than those of later-L dwarfs - the so-called J-band bump; further problems arise from the large dispersion of certain colors as a function of spectral type as well as discrepancies between the optical and nIR derived spectral types of some objects. These questions are likely related to the atmospheric physics of ultra-cool BDs, and in particular to mechanisms of **dust clearing through specific weather patterns likely occurring in their atmospheres** (e.g. Morales-Calderon et al 2006, ApJ 653, 1454). The disk-averaged spectral energy distribution (SED) of ultra-cool BDs may indeed not be representative of any single region, suggesting that attempts at modeling their SED using a unique set of physical parameters (e.g. temperature, dust-settling properties, grain properties) are bound to be incomplete. For example, unresolved spectroscopy of Jupiter would not reveal the richness of its weather patterns and some basic properties would be missed with disk-averaged observations, e.g. the fact that most of the 5 µm flux comes from hot spots covering only ~10% of the disk.

First evidence that this is likely what happens comes from the observational fact that **ultra-cool BDs often exhibit photometric variability** at a level of a few % up to a remarkable 25% (Artigau et al 2009, ApJ 701, 1534, Radigan et al. 2012, ApJ, 750, 105). This variability is apparently due to a combination of rotational modulation and intrinsic evolution on short timescales, accurate multicolor photometric monitoring suggesting that it is indeed likely **caused by weather-like clearings in the dust-cloud deck** (e.g. Littlefair et al 2006, MNRAS 370, 1208). Unravelling the physics of these weather patterns and distinguishing between the several existing theoretical scenarios would require observations capable of localizing the dust clouds in BD atmospheres and following their rapid evolution with time.

Since the nearest BDs have apparent diameters <1 mas, no existing (nor planned) instrumentation will be able to provide soon actual images of their surfaces. Indirect (i.e. Doppler) imaging through high-resolution nIR spectroscopy is a very attractive & viable approach to attempt mapping weather patterns of BDs; most BDs are indeed rapid rotators and often exhibit rotational modulation, both photometrically & spectroscopically, providing ideal conditions for Doppler imaging. Though not yet applied to stars cooler than mid-M due to their intrinsic faintness at optical wavelengths, Doppler imaging of BDs in the nIR is feasible, opening a new window for studying chemical inhomogeneities in their atmospheres.

High-resolution nIR échelle spectroscopy of BDs is obviously ideal in this respect. Thanks to the large multiplex gains provided by the many molecular lines (e.g. from CH_4, H_2O, CO, FeH) available in the wide single-shot spectral domain, one can boost the resulting S/Ns up to values of ~500 (per 2 km/s pixel) that indirect imaging typically requires. For instance, exploiting all CH_4absorption lines in the H & K bands (e.g. through cross-correlation techniques) can enhance S/Ns by factors of ~20; peak S/Ns of ~30 (per 2 km/s) pixel in raw spectra are thus sufficient.

Reaching S/N~30 (per 2 km/s pixel) in less than 900 s (to freeze rotation to ~1/10 th of a cycle, BDs typically rotating in a few hours) requires J<14 and K<12.5. About **70 early-L, 4 late-L & 3 T single BDs are accessible from CFHT**, from which the ~10 exhibiting largest photometric rotational modulation & high enough rotational broadening in line profiles can be selected for this study; monitoring each of these for about 6 hr per night (i.e. 2 rotation cycles) for 4 successive nights (to follow-up weather patterns) will typically require ~6 nights/yr for ~5 yr. The first Doppler map of a brown dwarf has recently been obtained on Luhman 16b, a T0 dwarf 2pc from the Sun. The brown dwarf has a 5h rotation period and displays >10% photometric variability (Biller et al. 2013, ApJ, 778, 10). Crossfield et al. 2014 obtained time-resolved CRIRES observations centered on the CO bandheads over one rotation period and were able to recover the first crude temperature map of a brown dwarf (see Figure 5.2). The authors highlight the necessity for broader wavelength coverage for that type of measurements, such as the one provided by SPIRou, both to increase the signal-to-noise from additional features included in LSD, and to construct maps of different chemical species.

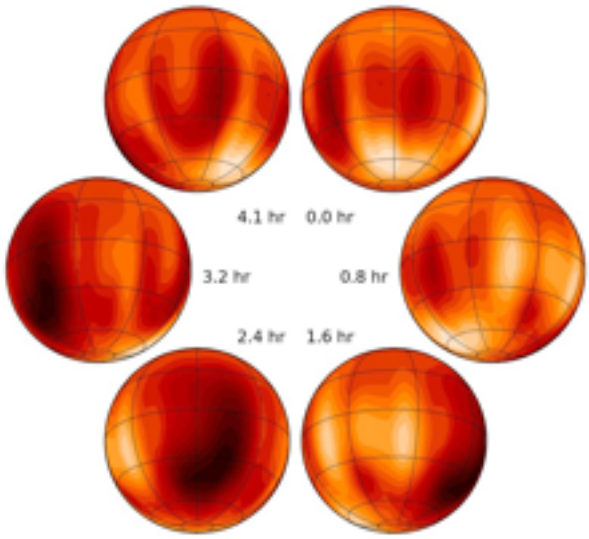

Fig 5.2 : Doppler imaging surface temperature map of Luhman16b obtained by Crossfield et al. 2014 in using CRIRES/VLT. More accurate surface maps could be recovered for tens of L dwarfs and a handful T dwarfs with SPIRou, benefiting from the broader wavelength coverage of SPIRou. This would allow a direct comparison between global SED properties and surface features for these objects.

5.3. Cool magnetic spots on active stars

Cool stars like the Sun host dark spots & magnetic fields at their surfaces. Their periodic photometric, spectroscopic & spectropolarimetric changes are usually interpreted as the signature of cool spots & magnetic regions coming in and going out of view of an Earth-based observer; in particular, time resolved sets of line profiles collected throughout complete rotation cycles are very sensitive tracers of how spots & fields are distributed over the surfaces of rotating active stars (e.g. Donati & Landstreet 2009, ARA&A 47, 333), offering a smart way of investigating activity cycles in stars other than the Sun through their surface brightness distributions, large scale field topologies and their evolution with time.

However, at visible wavelengths, cool starspots are mainly detected by their lack of continuum photons with respect to nearby regions at photospheric temperature. In Sun-like stars (of spectral types GK), the temperature contrast between spots and the surrounding quiet photosphere is indeed ~1,500 K (e.g. Berdyugina 2005, LRSP 2, 8), implying a 10-fold brightness contrast in V; this comparative lack of continuum photons is precisely what generates the line profile bumps & photometric modulation through which starspots reveal their presence. As a consequence, little information about the physical properties of these spots can be derived apart from their temperature & spatial distribution; in particular, measuring field strengths within cool spots (requiring a spectrum of the emitted light) is virtually impossible, except for the brightest stars.

At nIR wavelengths, the spot to photosphere brightness contrast is much smaller, by typically a factor of 4 in H, than in the visible; **nIR spectra are thus far more adapted for studying the intrinsic properties of starspots**, and in particular their magnetic field strengths & orientation thanks to the higher Zeeman sensitivity that longer wavelengths bring. For instance, this can be achieved by looking at Zeeman signatures from lines with different excitation potentials, e.g. formed selectively in photospheres & spots only. Looking for large-scale velocity fields within large starspots (e.g. similar to Evershed flows on the Sun) and deriving quantitative observational estimates of how much convection & turbulence are suppressed in these regions are other potentially very promising applications, for which high spectral resolution is crucial. Hundreds of bright active stars (i.e. with H<7) of different spectral types - essentially all those already studied at optical wavelengths - are available for the new nIR spectropolarimetric observations suggested here. Such detailed studies of starspots on a few selected targets will ideally complement the stellar variability statistics obtained on thousands of cool stars by photometric missions such as Kepler (e.g. Basri et al. 2011, AJ 141, 20).

Selecting ~20 of them, with different surface temperatures (i.e. masses) & activity levels (i.e. rotation rates) and carrying out a detailed monitoring of their Zeeman signatures should reveal fundamental characteristics of starspots and allow fruitful comparisons with their solar analogs. This typically requires ~10 spectra per star evenly sampling the rotation period (for tomographic imaging), each at high S/N (~500 per 2 km/s pixel, in order to detect Zeeman signatures from individual spectral lines and requiring ~1 hr of observing @ H=7); altogether, it yields a total of ~25 nights.

5.4. Ultra-cool spectroscopic binaries & the formation of brown dwarfs

Fifteen years after the unambiguous discovery of brown dwarfs, hundreds of them are now known, and their physical properties are increasingly better understood

(e.g. Chabrier & Baraffe 2000, ARA&A 38, 337). Their formation mechanism, and that of the very-low-mass stars (with which they form a continuum), remains on the other hand a topic of very active discussion. Given the typical thermal Jeans mass in molecular cloud cores (~1 $M_\odot$), quasi-static gravitational collapse is not expected to form objects very much less massive than the Sun.

Star formation however is not likely to be quasi-static, and a number of mechanisms have been proposed for forming very-low mass dwarfs, e.g. turbulent fragmentation of molecular clouds, fragmentation of prestellar cores, disc fragmentation, ejection of protostellar embryos (e.g. Whitworth et al 2007, PPV). In this respect, the multiplicity statistics of ultra-cool (i.e. late-M, L & T) dwarfs provide a key diagnostic of the relative contributions of these various modes of brown dwarf formation, each of which is expected to produce distinct multiple star fractions, different distribution functions for separations & mass ratios, and distinct variations of these quantities with primary mass.

From the point of view of observations, high-resolution imaging surveys have found a few dozen ultra-cool field binaries, suggesting that up to ~15 % of the ultra-cool field dwarfs have visual companions at a distance of at least ~1 AU (Bouy et al 2003, AJ 126, 1526; Burgasser et al 2003, ApJ 586, 512). The detection of binaries with smaller separations, out of reach of imaging surveys, requires collecting nIR spectra and tracking the periodic RV variations induced by orbital motions (at a RV precision of a few 0.1 km/s).

By monitoring the RVs of the 100 brightest LT dwarfs, e.g. for detecting the giant planets they potentially host (see Sec 3.5), one can quantitatively estimate at the same time (as a free by-product) **how frequent spectroscopic (i.e. close) binaries are among ultra-cool dwarfs**, thus usefully complementing visual binary rates derived from imaging surveys.

5.5. The formation of massive stars

The formation of massive stars is a vigorously debated topic. As opposed to low- and intermediate-mass stars, massive protostars are so luminous that their radiation pressure & powerful winds can potentially stop the accretion flow, suggesting at first that different processes (e.g. coalescence) are required to form massive protostars. Recent 3D hydrodynamical simulations including radiative feedback (Krumholz et al 2009, Science, 323, 754) however indicate that ionizing radiation can escape through lobes between which accretion can proceed. To confirm that the accretion scenario is indeed valid, observations of accreting protostars are necessary. Being by nature surrounded by (atomic & molecular) gas & dust, massive stars in the making are usually hidden by several magnitudes of extinction, rendering them unobservable at optical & UV wavelengths (where they emit the bulk of their light). Detecting & observing them in the nIR, where their continua are still significant and the contribution of heated dust not overwhelming, is the best way to characterize their properties. For instance, nIR imaging surveys (e.g. SPITZER/GLIMPSE) revealed several star forming regions showing bubbles/H II regions blown by stellar winds of newborn massive stars (e.g. Churchwell et al 2007, ApJ 670, 428).

Whereas accretion on massive protostars is often inferred from nIR excesses, observations of inflows remains the most unambiguous evidence. In particular, photospheric lines may provide a definite proof, clumps of material falling onto the stellar surface modifying the opacities and thus the shape of lines. Time series of selected photospheric lines should thus reveal the presence of inflows through the

variability they can generate in the red wings; this requires in particular high S/N (~100), high-resolution profiles of, e.g. Brackett & He lines (in the HK spectral bands). At even earlier phases of evolution, massive stars appear as young stellar objects (YSOs) spectroscopically characterized by several emission features (e.g. H_2, Brγ), some of them (CO bandheads) attributed to a circumstellar disc. From the morphology of the emission profiles (broadened or split by rotation), one can estimate the rotation rates of these putative structures - and thus the mass of the central protostar mass as well (e.g. Bik et al 2006, A&A 455, 561). High-resolution (>10,000) spectra of CO bandheads (in the K band) are thus essential to constrain the properties of young & potentially massive stars in the making.

About 2-4 CO-emitting YSOs are expected in many of the few hundreds of bubbles/H II regions discovered by the SPITZER/GLIMPSE survey. Located mostly at ~4 kpc, these YSOs have typical K magnitudes of 10-14, with the most massive ones supposedly being the brightest. By concentrating on the few tens of YSOs with K<11, **high-resolution nIR spectroscopy can provide convincing evidence that accretion is involved in the formation of massive stars**. Surveying ~80 stars (about 10 stars in 8 different star forming regions) requires ~10 nights.

5.6. Circumstellar environments: chemistry, kinematics & geometry

Circumstellar environments combine high temperatures & densities, leading (as a result) to a very active chemistry and to the formation of molecules & dust. These environments can thus be used to probe chemical evolution associated to stellar formation; moreover, the composition & excitation of matter retrievable from spectroscopic fingerprints can be used to characterize the local physical & chemical conditions (e.g. radiation field, density, grain temperature) and to constrain accretion disc geometries & stellar formation scenarios.

nIR wavelengths are particularly well suited in this purpose. In YSOs for instance, the luminosity contrast between the central star & the surrounding accretion discs is much smaller than at optical wavelengths, making their direct spectral study much easier. High-resolution nIR spectra also include a number of spectral proxies capable of probing massive star formation (see Sec 5.5) and can provide complementary data to radio-telescopes such as ALMA or NOEMA.

More specifically, it will allow to probe several gas & dust tracers, e.g.:

- hot molecular ro-vibrational emission from H_2, H_2O, CO observed in the inner disc of massive YSOs (e.g. This & Bik 2005, A&A 438, 557); in particular, the overtones & combination modes of many molecules & radicals (accessible in the nIR domain) can be used to trace the first steps in dust nucleation; high-spectral resolution (~5 km/s) is needed to analyze the fine structure of these bands and the kinematics of the studied regions, while the wide spectral coverage allows one to constrain all issues (chemistry, kinematics & physical conditions) simultaneously;

- molecular ices showing nIR combination bands, e.g. solid CH_3OH (methanol) @ 2.27 μm & solid NH_3 @ 2.21 μm (Taban et al 2003, A&A 399, 169), both showing relatively narrow (i.e. 0.03 μm) structures easily accessible to high-resolution échelle spectroscopy; for these solids, searching for combinations modes is often the only way of estimating their abundances (their fundamental bands being hidden by saturated fundamental modes of other species, e.g. NH_3 bands hidden by H_2O bands).

Searching for the nIR (1.68 μm) overtone of the 3.3 μm band of polycyclic aromatic hydrocarbons (PAHs) already detected in emission in a young planetary nebula (Geballe et al 1994, ApJ 434, L15) is also possible and potentially very fruitful

for probing the size of the PAH population. High-resolution spectroscopy is mandatory for properly removing the contamination by gas lines from the circumstellar material, from the star itself & from the atmosphere.

Circumstellar environments, and in particular their geometries, can also be studied through polarization in line profiles - especially when the objects of interest are far too distant to be investigated through direct imaging techniques, e.g. protostellar dust cocoons, accretion discs & jets around YSOs, winds around massive stars, excretion discs around Be stars, extended envelopes around cool giants. By looking at polarization structures in line profiles, and in particular at how the scattering polarization of emission lines formed in specific regions of the spatially-extended circumstellar environment (e.g. Paβ, Paγ & Brγ) differ from that of the continuum (mostly produced from the point-like central star), one can investigate for instance the localization, the geometry and to some extent the physical properties of the scattering medium at spatial scales that interferometry cannot yet reach (e.g. Takami et al 2006, ApJ 641, 357; Vink et al 2005, MNRAS 359, 1049; Kurosawa et al 2005, 358, 671). In particular, nIR spectropolarimetry will help alleviate limitations of existing studies, e.g. on the star-disc interaction zone and the inner disc regions where protoplanets are expected to form and/or settle.

Such studies are original and powerful means of investigating the geometry and physical conditions in a wide range of circumstellar environments. In addition to **polarimetric capabilities** (in both circular & linear polarizations), they require access to **a large single-shot spectral domain** to be able to monitor simultaneously a large number of proxies, and to **the K band in particular** containing several of the main ones (e.g. Brγ, CO bandheads). Means of filtering out linear polarization may be helpful as well for double-checking the reliability of weak circular polarization signatures from sources exhibiting strong levels of linear polarization.

We estimate that ~10 nights as a whole is needed to cover the various topics of this research thread.

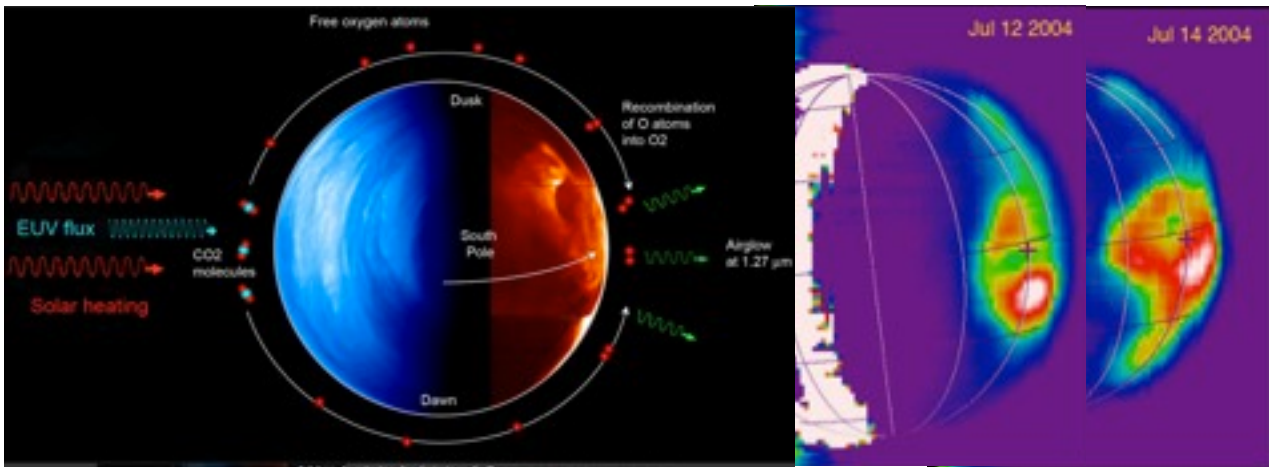

Fig 6.1: Schematic of O_2 ($a^1\Delta_g$) oxygen non-LTE airglow production. Photo-dissociation of CO_2 in the upper atmosphere on Venus's day side releases oxygen atoms that recombine on the night side (left), producing the non-thermal, highly-variable nIR O_2 fluorescence emission (right, from Bailey et al 2008, Icarus 197, 247).

6. Planetary atmospheres

The current & following sections present 5 different programs for which a high-resolution nIR spectropolarimeter/velocimeter can provide valuable results in a few very specific topics. We estimate that a typical amount of ~**10 nights per year over 5 years** is needed (as a whole) to carry these various programs; given this moderate amount (per program, and with respect to most programs described above in particular), we only provide below the main ideas underlying the programs and skip specific details on observing samples.

6.1. The atmospheres of solar-system planets: chemistry & winds

Studies of the dynamics & chemistry of both dense & thin solar-system planet atmospheres can strongly benefit from high-resolution nIR spectra collected over a wide single-shot spectral domain, through the many molecular bands available in the nIR window; **in particular, detecting the presence & measuring the abundance of trace species appears as a powerful way of probing the atmospheres/envelopes of both telluric & giant planets** and potentially those in the distant solar system as well. The important role of interactions between atmospheric volatiles, planetary interiors & climate is increasingly acknowledged. Accurate RVs may also characterize latitude-dependent wind fields at various altitudes, as well as their variation with time, in various solar-system planet atmospheres (as described in a few examples below).

On Venus, the composition of the deep atmosphere is constrained by surface/atmosphere interactions & thermochemical cycles, while the composition above the clouds is affected by meteorological & photolytic processes. High-resolution nIR spectroscopy can probe the upper atmosphere of Venus on the dayside and its deep atmosphere on the nightside; with a wide single-shot spectral coverage, one can address these couplings, e.g. the correlation between the vertical distribution of H_2O (as measured from the observation of water vapor in JHK bands, e.g. Bézard et al 2009, JGR 114, E00B39) and the local cloud cover.

Uranus & Neptune are icy giants; they remain poorly characterized in the absence of detailed spacecraft exploration. A fundamental issue is to better understand the remarkable differences between Uranus & Neptune in terms of composition & internal

structure. Spectroscopic estimates of the abundances of deep species like CO, CH_4 & CH_3D (K band) are available, but remain inaccurate given the very crowded spectra. Using high-resolution spectra covering a wide single-shot domain, improved abundance determinations can be obtained, yielding new insights on internal convection & meteorology.

Finally, monitoring of the abundance of CH_4, CO (K band), SO_2 and possibly other species in the tenuous atmospheres of Triton, Pluto & Io will also provide new views on the nature of surface/atmosphere interactions & seasonal effects (e.g. Lellouch et al 2009, A&A 495, L17).

Regarding atmospheric dynamics, high-resolution optical spectroscopy has proved a powerful way of measuring absolute wind velocities in planetary atmospheres (e.g. Widemann et al 2008, P&SS 56, 1320). **Extending these measurements to the nIR with improved RV precision will allow one to determine wind variability & latitudinal structure as a function of altitude**, and to compare/correlate these results with winds measured from cloud motion.

6.2. Airglow & aurorae of solar-system planets

Airglow is caused by various processes in the upper atmospheres of solar-system planets, e.g. the recombination of ions and luminescence caused mainly by oxygen & nitrogen reacting with hydroxyl ions at altitudes of a few hundred km. Planetary airglow is a powerful way of remotely probing planetary upper-atmospheres, with airglow morphology, brightness & temporal variations providing key observations regarding atmospheric composition, temperature structure, transport processes & their response to solar photon & particle inputs. For selected species, the distribution of ro-vibrational bands (accessible with high-spectral resolution) provides information on the rotational temperature, while direct Doppler wind measurements map global circulation patterns & their variability.

In the mesosphere of Venus, the O_2 airglow @ 1.27 µm is the most intense non-LTE emission; it is produced by the recombination of oxygen atoms created by photo-dissociation of CO_2 & CO on the dayside and transported by mesospheric winds across the terminator to the nightside (see Fig 6.1). It belongs to the $a^1\Delta_g - X^3\Sigma_g$ IR system and corresponds to a transition with a radiative lifetime of about 70 min (e.g. Gerard et al 2009, JGR 114, E00B44); its complex structure & extreme temporal variability are however still poorly understood. The mesosphere of Venus (extending typically from 70 to 110 km) appears as a transition region between the troposphere (0-70 km) dominated by retrograde super-rotation, and the thermosphere (110-250 km) in which diurnal temperature contrasts drive a predominantly subsolar-to-antisolar circulation. **Through sequential observations of the O_2 airglow emission - and in particular its rotational temperatures & Doppler shifts - over the night side, high-resolution nIR spectroscopy & velocimetry of Venus is ideal for monitoring the thermal structure, composition & dynamics of the mesosphere.**

For outer giant planets, H_3^+ emission @ 2.09 µm & H_2 emission @ 2.12 µm (and their correlation) can efficiently **probe the energetics & dynamics of upper atmospheres, as well as the coupling with magnetospheres**. Large amounts of H_3^+ are formed in the auroral regions of Jupiter, Saturn, Uranus & Neptune through the ionization of molecular hydrogen by energetic electrons precipitating along magnetic field lines (e.g. Raynaud et al 2004, Icarus 171, 133); emission intensity, temperature & column density can thus be simultaneously monitored using high-resolution nIR

échelle spectra. H_3^+ emission can also trace winds through accurate velocimetry (e.g. Rego et al 1999, Nature 399, 121).

Planetary emission lines can also be partially polarized, as recently demonstrated in the particular case of the Earth (e.g. Lilensten et al 2008, GRL 35, L08804) and Jupiter (Barthélémy et al 2010, A&A submitted). Even though the exact polarizing mechanism depends on the specific line, polarization is very often a proxy of possible anisotropies within the emission region, and in particular those related to the presence & local configuration of magnetic fields. Spectropolarimetric capabilities are thus potentially interesting.

6.3. Exoplanet atmospheres

Now that hundreds of exoplanets have been found, including Super-Earth in habitable zone. Detecting potential bio-signatures from these habitable exoplanets appears as one of the most exciting challenges of the new century. Although life abounds in hidden places of the Earth, photosynthetic organisms - at the basis for nearly all life on Earth - produce some of the strongest indicators of life in abundances that can be detected astronomically. Detecting photosynthetic life on exoplanets requires obtaining their spectra (and in particular that of their atmospheres), from which distinct reflectance spectra of photosynthetic organisms or gaseous products of primarily biogenic origin can in principle be identified (e.g. Tinetti et al 2006, ApJ 644, L129). This is obviously a far-reaching aim for future generation exobiology missions (such as Darwin/ESA & TPF/NASA); present observations can nevertheless start contributing through early explorations of exoplanet atmospheres and in particular participate to JWST programs aimed at detecting biomarkers on planets around M dwarfs (Seager et al 2009, A&SSP, p123).

Whereas atmospheres of solar-system planets are routinely observed from both space & ground, those of exoplanets are more elusive & tricky to investigate. The atmospheres of transiting close-in giant planets can be scrutinized, either by transmission (when the planet atmosphere crosses in front of its host star) or by occultation (when the day-side planetary hemisphere is occulted by the host star) through comparisons with out-of-eclipse spectra. Following this dual strategy and using the nIR spectrophotometers aboard Spitzer & HST, several molecules (including H_2O, CH_4, CO, TiO, VO) have possibly been detected in the atmosphere of the close-in giant planet HD 189733b (e.g. Swain et al 2008, Nature 452, 329; Désert et al 2008, A&A 492, 585; 2009, ApJ 699, 478; Tinetti et al 2010, ApJ 712, L139).

High-resolution nIR spectroscopic monitoring of close-in exoplanets are able to resolve molecular bands into individual absorption lines. Such observations have the capacities to detect absorption by molecule during transit and can also potentially reveal the day-side spectra of their atmospheres, e.g. though signal enhancement techniques & matched filter analysis, even if the planet is not transiting (Barnes et al 2008, MNRAS 390, 1258; Barnes et al 2010, MNRAS 401, 445). Snellen et al. (2010, Nature 465, 1049) allowed to start characterizing the exoplanet atmosphere with a ground-based instrument (CRIRES@ESO) in detecting carbon monoxide lines during a transit of HD209458b. Interestingly the observations possibly indicating day-to-night winds. CO lines was also been detected in the day-side thermal emission of the non-transiting planet Tau-Boo b (Brogi et al. 2012 Nature 486, 501, Rodler et al. 2012 ApJ 735, L25) and in the transiting planet HD189733b (de Kok et al. 2013a, A&A 554, 482). For this last planet Birkby et al (2013, MNRAS 436, L35) also found water vapor

but in using observation in L-band. Such measurements reveal the temperature profile of exo-planets atmosphere and can also determine relative abundances of gases.

De Kok et al. (2014, A&A 561, 150) perform simulations of high-resolution spectroscopic observations to identify new ways of increasing the planet signal during transit or for thermal emission. They identify SPIRou **should be able to provide a valuable contribution to this field** thanks to its wide single-shot spectral domain & high throughput on the one hand (increasing the amount of information available for such studies) and to its exceptional stability (allowing a cleaner separation & subtraction of stellar & telluric lines from the planetary signal to be detected).

These techniques can also potentially be used to search for **aurorae in the atmospheres of close-in giant exoplanets around M dwarfs**, e.g. by focussing specifically on H_3^+ emission @ 2.09 µm. In particular, such observations could provide constraints on the magnetic field at the surfaces of exoplanets, e.g. in conjunction with simultaneous radio observations with LOFAR.

7. Galactic & extragalactic astronomy

7.1. Chemical evolution & kinematics of the Milky Way

Understanding the chemical evolution of galaxies starts with unveiling the physics of the main galactic chemical factories, i.e. the stars. In this respect, high-resolution nIR spectra offer a unique opportunity to study the chemical properties of stellar populations & stellar evolution; in particular, the chemical abundances of CNO elements & their isotope ratios can be derived, in spectra of cool stars, from the numerous nIR lines of the C_2, CN & CO molecules, allowing one to trace the chemical evolution resulting from, e.g. internal mixing and/or nucleosynthesis. Stars ascending the red giant branch (RGB) & evolving on the asymptotic giant branch (AGB) are the main targets for such studies, as their surface chemical compositions is strongly modified during their evolution. Other metals with specific sensitivity to the star-formation history & the initial mass function, such as iron-peak, odd-Z, & alpha-elements can also be studied in the context of galactic archeology.

A detailed understanding of element nucleosynthesis is necessary to reconstruct the history of a stellar population through its chemical evolution. However, despite the bonanza of abundance studies performed so far, the origin of some elements remains poorly known. The best example among the light metals is fluorine, whose production sites are rather obscure, reflecting both observational & theoretical uncertainties. The only stable isotope of fluorine (^{19}F) is not easily produced in stars; moreover, F lines are absent in optical spectra. For cool stars, however, the HF molecule (showing nIR lines @ 2.34 µm) is easily formed, opening the possibility to study fluorine abundances and to discriminate between the various nucleosynthetic options for producing fluorine (e.g. Abia et al 2009, ApJ 694, 971).

Low- and intermediate-mass RGB stars are another potentially significant contributor to galactic chemistry. As they undergo mixing processes, RGB stars bring to their surfaces freshly synthesized nuclides, subsequently expelled into the ISM through winds that grow stronger as evolution proceeds. The precise role played by RGB stars in the chemical enrichment of the Universe is however vigorously debated, reflecting partly the still uncertain efficiencies of the mixing processes (and their dependence on stellar mass & metallicity); in particular, the respective impact of various mixing mechanisms (e.g. convection, diffusion, thermohaline mixing) is indeed

still debated, preventing in addition any accurate study of the initial chemical abundances of several elements in distant stellar clusters. A better knowledge of RGB mixing is therefore urgently required. Using nIR high-resolution spectra of CO bandheads @ 2.35 µm, carbon isotopic ratios at the surface of near-RGB stars can be determined more accurately (e.g. Recio-Blanco & de Laverny 2007, A&A 461, L13), putting constraints on various mixing models, e.g. meridional circulation & thermohaline mixing.

Galactic bulges are a key to galaxy formation; their origin & history remain however poorly understood. In the particular case of the Milky Way, detailed chemical composition studies of bulge stars, carrying characteristic signatures of processes enriching the interstellar gas, are essential; in particular, abundance ratios are sensitive to the time-scales of star formation, to the initial mass function, and may disclose relations between different stellar groups. For instance, the mismatch between the present abundance results and the shape of the bulge suggests a more gradual merging or secular evolution, with contributions from the disk and on-going star formation. A systematic study of stellar abundances (e.g. O, C, N, Fe), abundance ratios (e.g. $^{12}C/^{13}C$, O/Fe) & kinematics of RGB stars in different parts of the galactic bulge through high-resolution nIR spectroscopy should be very fruitful. Obscuration towards the bulge is considerably reduced in the nIR, allowing one to access heavily reddened regions; nIR spectra also suffer much less line blending than optical spectra, yielding more reliable abundance estimates.

High-spectral resolution nIR spectroscopy can nicely complement the APOGEE (Apache Point Observatory galactic evolution experiment) mid-resolution (24,000) spectroscopic survey of 100,000 red giants (up to H~12.5), aimed at yielding the first large-scale, uniform, high-precision study of all stellar populations (bulge, disc, bar, halo) in the galaxy and at providing an unprecedented description of the Milky Way in terms of scope, richness & detail. Higher-resolution nIR spectra of a limited number of reference stars can in particular be very useful for calibrating abundances from mid-resolution spectra and for providing additional abundances (e.g. F, CNO isotopes).

7.2. Extragalactic astronomy

In galaxies other than our own, high spectral resolution can be used to partly compensate for the lack of spatial resolution and to reveal the intricate velocity structures of their inner regions (e.g. Pelat & Alloin 1980, A&A 81, 172; Cecil et al 2002, ApJ 568, 627). At a spectral resolution of about 70,000, however, only very few (nearby) extragalactic sources are accessible on a 4m telescope, the available flux being extremely low. There is still a few niches that can (and should) be exploited; in this respect, the nIR domain offers a number of interesting spectral diagnostics (e.g. H_2 emission, CO bandheads) that can help for studying both **the hot gas components** (and the underlying physical emission processes) as well as **the stellar populations** (e.g. age, metallicity).

NIR spectra at high-spectral resolution can reveal new information on **active galactic nuclei** (AGN), and in particular the physical status of the gaseous component in the central few hundred parsecs. In all cases, only a handful of objects would be accessible given the typical S/N ratios (about 50 per resolution element) needed for these studies in a few hours of integration time.

Studying **super stellar clusters** in nearby galaxies can also benefit from high-resolution nIR spectroscopy, making it possible to determine dynamical masses (through their velocity dispersion) as well as ages and metallicities; they can thus

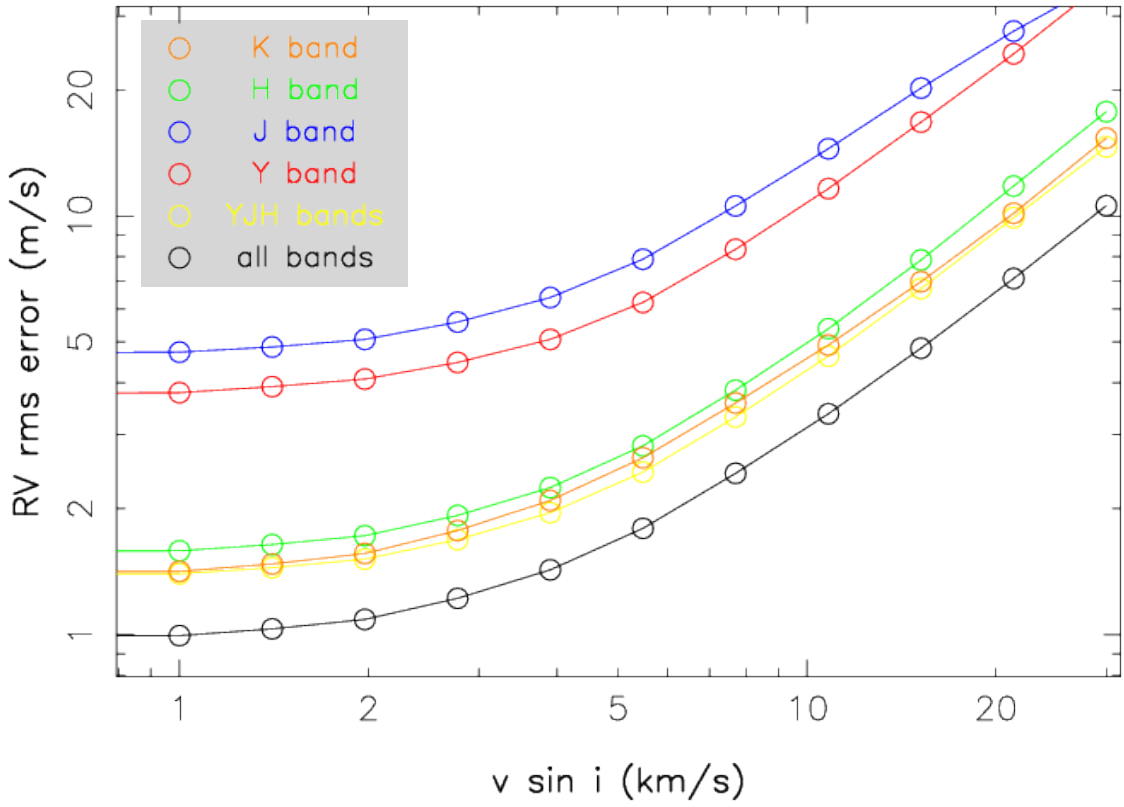

Fig 8.1: RV rms photon-noise error (in m/s) vs rotational broadening (v sin i) for a M7 dwarf (2,700 K) and for the different nIR bands (color curves), assuming a spectral resolution of 75,000 and a peak S/N of 160 per 2 km/s pixel. A RV precision of ~1 m/s can be reached at low v sin i's. **The K band** (orange) **is the main contributor to the RV precision and contributes almost as much as all other bands** (yellow). Without the K band, a twice longer exposure time would be required to reach the same RV precision.
Note that this estimate is likely pessimistic by potentially as much as a factor of 2, nIR synthetic spectra systematically under-estimating the strength of many molecular and even atomic features.

serve as unique probes of star-formation processes. In the youngest of such clusters, the so-called **emission-line clusters** (ELCs), massive gas outflows at supersonic velocities are detected (using Brγ, Gilbert & Graham 2003, IAU Symp 221, 63) that would be worth extensive observations at high-enough spectral resolutions.

Ideally, high-resolution spectra should be combined with spatially-resolved data in order to better understand the complex dynamics of these regions.

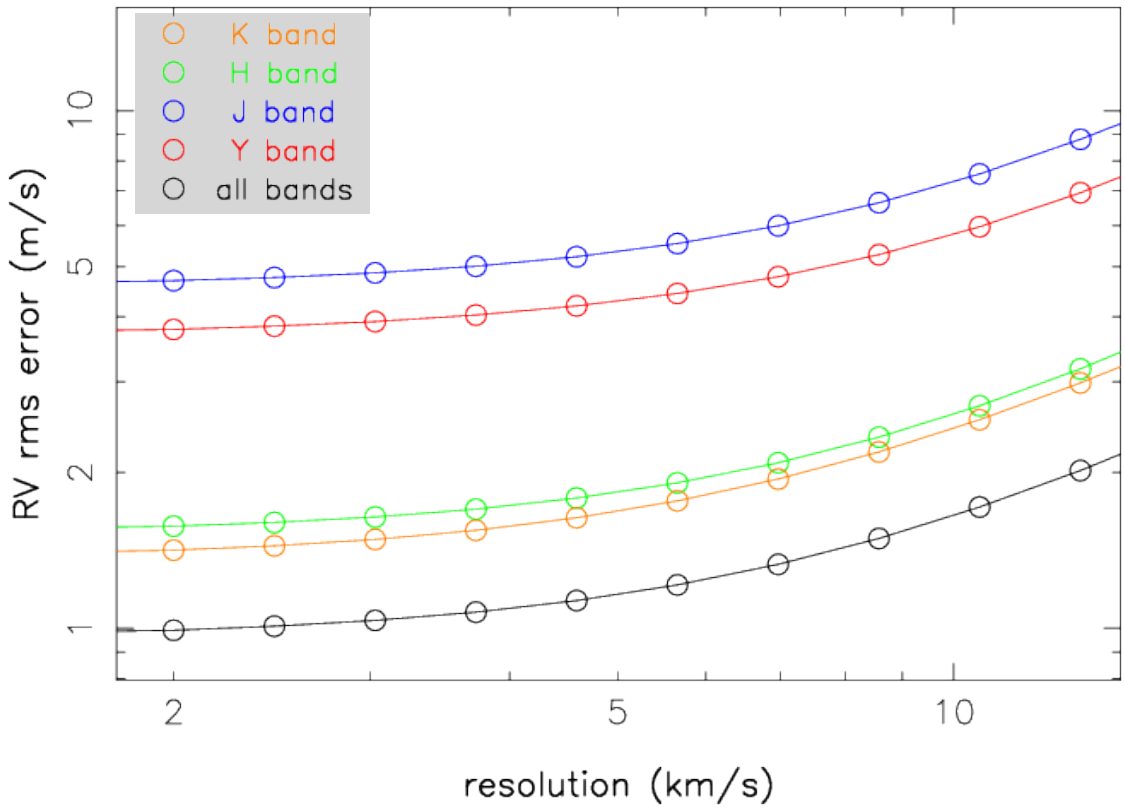

Fig 8.2: RV rms error (in m/s) vs resolution (in km/s) for a M7 dwarf (2,700 K) and for the different nIR bands (color curves), assuming a rotational broadening (v sin i) of 2 km/s and a peak S/N of 160 per 2 km/s pixel. The RV precision steadily decreases with increasing resolution (in km/s) and decreasing resolving power. At a resolution of 4 km/s (resolving power of 75,000), the RV precision is only ~10% lower than optimal, but ~15% & ~40% better than at resolutions of 6 & 9 km/s (resolving powers of 50,000 & 33,000).

8. Science requirements

We list here the main requirements that SPIRou must satisfy for successfully addressing all the science goals described in Secs 3-7. We list all requirements separately, describing in detail the most crucial ones, and finally summarize them at the end of this section.

8.1. Simultaneous spectral domain & the K-band

SPIRou must provide **nIR spectra covering the Y, J, H and K bands** (i.e. 0.98-2.35 μm). The vast majority of targets of interest are either very cool (e.g. late-M dwarfs) or embedded (e.g. class I protostars, suffering very large extinctions at optical wavelengths), with photon distributions peaking in this spectral range (see Fig 3.2).

To maximize data collection efficiency, SPIRou must provide as wide a simultaneous spectral domain as possible. The wider the spectral window, the more lines available for estimating RVs; moreover, **collecting the whole YJHK domain in a single exposure** with a static (non-tunable) instrument is far better (both for stability & efficiency) than covering it in several exposures with a tunable spectrograph.

As emphasized in the various sections, **including the K band is attractive for all science programs**. For velocimetry, it provides a lot more photons & spectral lines from which RVs are estimated; for late-M dwarfs in particular, **the K band is the main contributor to RV precision.** More specifically, we find that the YJHK bands

respectively contribute to the RV information content at a relative level of 8%, 7%, 40% & 45% respectively (with a relative precision of ~10%), and therefore that **the K band provides 40-50% of the overall RV content**, i.e. almost as much as all other bands together (see also Fig 8.1). In other words, the addition of the K band is almost doubling the overall RV efficiency (with respect to an H-band-limited instrument).

For stellar formation programs, **the K band gives a broad access to embedded protostars** that are barely accessible blue-ward of 2 μm (see Fig 4.3). For more evolved protostars and stellar magnetometry in general, **the K band offers maximum magnetic sensitivity over the YJHK window**, Zeeman splitting growing linearly in amplitude with wavelength with respect to line profile widths. More specifically, we find that the YJHK bands respectively contribute to the spectropolarimetric content at a relative level of 3%, 3%, 31% & 63% respectively (again with a relative precision of ~10%). This implies that adding in the K band enhances the instrument spectropolarimetric efficiency by a factor of ~3 (with respect to an H-band-limited instrument).

The cost of adding the K band is that the whole instrument must be installed in a cryogenic dewar (and not just in a vacuum tank as that of HARPS).

8.2. Spectral resolving power

For a large majority of science programs, **SPIRou must provide spectra at a resolving power of ~75,000**.

This is especially important for velocimetry, requiring spectral lines to be as sharp as possible to maximize their RV information content (e.g. Bouchy et al 2001, A&A 374, 733); for M dwarfs, whose spectra typically exhibit a rotational broadening of a few km/s and intrinsic line widths of ~7 km/s, a resolving power of >70,000 is appropriate (see Fig 8.2). At resolving powers <50,000, line blending becomes more severe and RV precision (at a given S/N) drops quickly, therefore requiring longer exposure times (by as much as ~30% & ~80% for resolving powers of 50,000 & 33,000, see Fig 8.2) for achieving the same RV precision; at resolving powers >100,000, the gain is only marginal except for the small fraction of very slow & inactive rotators (e.g. Reiners et al 2010, ApJ 710, 432).

For studying stellar formation and magnetic fields, resolving powers of >70,000 are also adequate; rotation of cTTSs being only moderate, resolving powers >50,000 are definitely mandatory for achieving reliable magnetic mapping of their large-scale fields. Whereas resolving powers of >100,000 can be useful for studying linearly polarized Zeeman signatures (featuring more complex shapes and much weaker amplitudes than circularly polarized ones), the prospect of reliably measuring them in these intrinsically very faint stars is rather dim.

8.3. RV precision

To achieve the science goals detailed in Sec 3, **SPIRou must be able to achieve a RV precision of 1 m/s**. As emphasized throughout Sec 3, SPIRou (as a velocimeter) will be largely dedicated for hunting Earth-like planets located within the HZs of, or even closer in, their host dwarfs, mandatorily requiring the ability of reaching a RV precision of ~1 m/s. Lacking this performance, a large fraction of the exoplanet science programs remains out of reach; for instance, a degraded RV precision of ~3 m/s would prevent detecting habitable super Earths around 0.3 $M_\odot$ dwarfs. In this context, SPIRou – while still capable of detecting giant planets around L & T dwarfs,

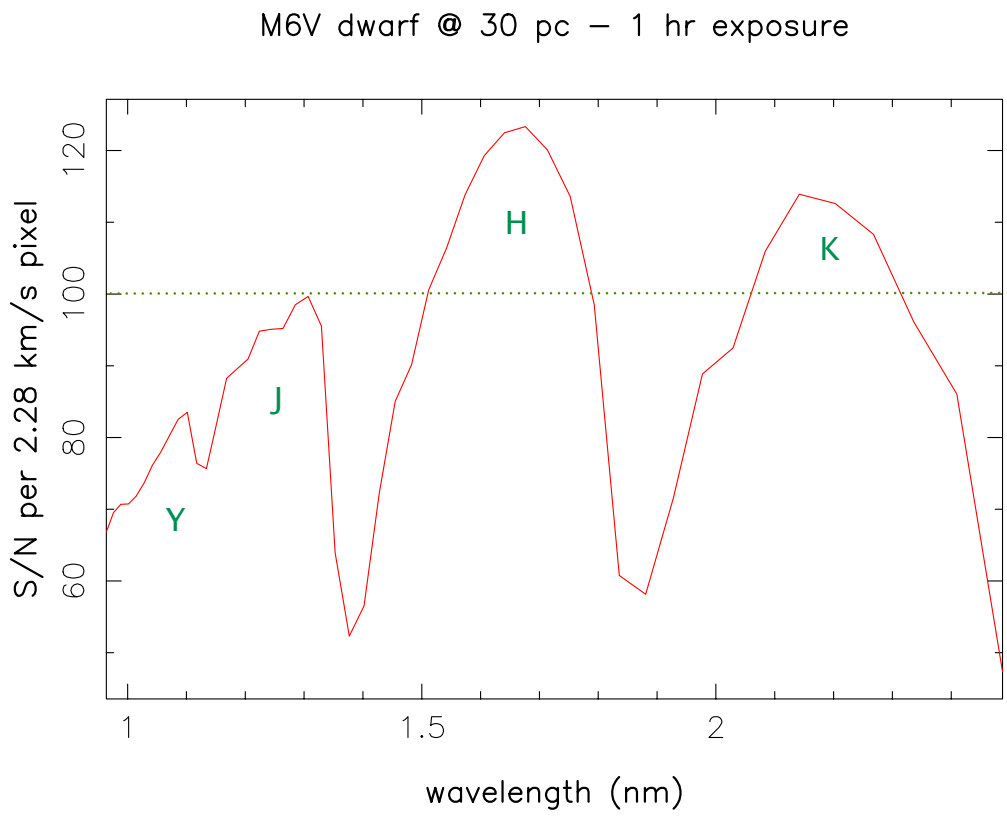

Fig 8.3: Estimated S/N (per 2.3 km/s pixel) as a function of wavelength for a 1-hr exposure with SPIRou on a M6 dwarf located at 30 pc (J=12, K=11), using a realistic instrument efficiency. The stellar photon distribution is taken from the NextGen models (Allard et al 1997, ARA&A 35, 137).

requiring a RV precision of ~10 m/s - would appear far less attractive in the long-term for this specific field of research.

To reach the 1 m/s precision, SPIRou must fulfill a number of critical conditions. The first one is to ensure that spectral sampling at the detector level is appropriate. Numerical simulations and experimental tests with ESPaDOnS@CFHT and NARVAL@TBL demonstrate that, for spectral bins <2.5 km/s, the sampling contribution to the RV error budget remains <0.25 m/s.

SPIRou should be as stable as HARPS (showing drifts of < 1m/s per night), requiring no simultaneous RV reference throughout a complete night and only using the RV reference to monitor the small night-to-night drifts (e.g. ~3 m/s per week on HARPS). This mandatorily requires the whole spectrograph to be included in a cryogenic dewar, with a very stable temperature control to minimize spectral drifts within observing nights.

SPIRou also needs to include **a very accurate & stable RV reference** for monitoring potential long-term and short-term RV drifts. In particular, this reference should ideally feature numerous (unsaturated) spectral lines more or less evenly spread throughout the whole YJHK spectral window, providing a RV precision of <0.45 m/s that can reliably demonstrate the RV performance of SPIRou; U/Ne lamps, thermalized Fabry-Perot etalons or comb lasers are interesting options in this respect. SPIRou must also implement the possibility of recording spectra of the RV reference simultaneously with stellar spectra throughout observing nights, even though SPIRou should be stable enough to avoid using it in normal operation.

SPIRou must also ensure that **light injection within the instrument**, and in particular within the spectrograph, **is well centered & very stable at all wavelengths** and that the RV impact of residual illumination offsets/changes are minimal**.** In this goal, ensuring that light injection is achromatic (to within ~0.05" at the instrument entrance pinhole, using an atmospheric dispersion corrector or ADC) is worthwhile. Stabilizing the stellar image (to within ~0.05" via a tip/tilt module) is also desirable. Scrambling the entrance image both azimuthally & radially (e.g. by factors of >1000) is necessary to reach the required RV precision, e.g. using the improved scrambling performance of the fiber systems currently developed & tested for optical velocimeters (e.g. HARPS). Last but not least, the spectrograph response should also be very weakly sensitive to pupil illumination changes (e.g. resulting from imperfect scrambling of the input image) and thus exhibit a very low level of asymmetric aberrations.

Since a majority of late-M stars (our most promising candidates for detecting super-Earths, see Sec 3.2) are active, **SPIRou must implement a convenient way of removing most of the RV activity jitter** (much smaller in the nIR than in the visible, see Sec 3.7) **by carrying out simultaneous spectropolarimetry** of all targets (see Sec 8.4). This procedure will allow modeling the large-scale magnetic topologies of the surveyed M dwarfs (see Sec 5.1) and filter out the resulting activity jitter using analytical relationships empirically determined from standard M stars of various activity levels (see Sec 3.7).

8.4. Polarimetric performance

Spectropolarimetric capabilities are absolutely essential for carrying out all forefront science goals of Sec 4. In particular, monitoring Zeeman signatures and their rotational modulation will give access to the large-scale field structures of cTTSs, protostellar accretion discs and red/brown dwarfs (see Secs 4 & 5.1) using magnetic imaging tools (e.g. Donati & Landstreet 2009, ARA&A 47, 333). It will also enable to **filter out most of the RV jitter from active M dwarfs** (see Sec 3.7) and thus to enlarge the sample on which Earth-like planets can be looked for. **SPIRou must carry-out spectropolarimetry at all times** to allow detecting circularly polarized Zeeman signatures of all surveyed targets and therefore to tackle multiple science goals simultaneously (e.g. RV & magnetic field surveys of late-M dwarfs).

To allow polarization signals in line profiles to be detected down to a precision of

specifications	required	supporting	unrelated
simultaneous spectral domain & K band	**3, 4**, 5-7		
R ~ 75,000	**3, 4**, 5, 6		7
RV precision <1m/s	**3**, 6		**4**, 5, 7
polarimetric performance	**4**, 5	**3**	6, 7
instrument sensitivity	**3, 4**, 5, 7	6	
observational efficiency	**3, 4**	**3**	
sky coverage	**3, 4**		

~10 ppm (e.g. through multiline techniques), and in particular to suppress to first order all potential sources of spurious polarization signals, **SPIRou must feature 2 separate channels for simultaneously collecting light from orthogonal**

polarization states, with the possibility of switching back & forth the role of both channels during observations (e.g. Donati et al 1997, MNRAS 291, 658). SPIRou must also implement specific observing & reduction procedures optimizing the collection & extraction of polarization spectra.

Given that most science programs are primarily interested in circular polarization, the polarimetric analysis must be achromatic enough to **maintain crosstalk between linear & circular polarization states at <2%** for minimizing the number of individual sub-exposures (typically 4) that are necessary to extract polarization spectra and avoid, e.g., high levels of linear polarization in line profiles to contaminate the weak circular polarization signatures to be detected.

8.5. Instrument sensitivity

Most key science programs critically require one to collect spectra with **S/N~100 (per ~2 km/s pixel) on stars with J~12 and K~11 in 1 hr**. This performance, corresponds to an average overall instrument throughput of ~15% (detector included).

The predicted S/N curve as a function of wavelength for a 1-hr exposure on a M6 dwarf at 30 pc (J=12, K=11) is shown on Fig 8.3, demonstrating that the main scientific goals of Sects 3 & 4 are perfectly realistic.

8.6. Observational efficiency & sky coverage

Finally, SPIRou should feature an observational efficiency of >70% and >90% for 15-min and 1-hr exposures respectively. This corresponds to overheads per exposure (due to, e.g., telescope pointing, target selection, instrument setup, detector read out) of <5 min - already verified in most QSO observations at CFHT. Any additional gain on the observational efficiency will further improve the overall duty cycle of the large RV & spectropolarimetric surveys planned with SPIRou - especially for exposures shorter than 10 min on bright stars.

SPIRou must also be able to access stars in the sky up to a zenithal distance of 70° (corresponding to an airmass of 2.5) so that variable stars can be accessed for as wide as possible a visibility window whenever visible. This is crucial for all RV & spectropolarimetric programs, depending a lot on the density of the rotational / orbital phase coverage.

8.7. Summary

We recall here the **full list of specifications** derived from the main science programs on which SPIRou will focus on:

★ the simultaneous spectral domain must include the YJHK photometric bands, i.e. cover the whole 0.98-2.35 μm range; in particular, the K band crucially improves contributes to most science programs;

★ the resolving power must be >70,000 (goal 75,000);

★ the RV precision must be better than 1 m/s; this implies in particular that the image at the entrance of the spectrograph must be stabilized as much as possible (e.g., by using fibers) and that reliable RV references are available on both short and long timescales;

★ the instrument must include an achromatic, dual channel polarimeter, with swappable channels to achieve accurate & reliable polarimetry; all polarimeter & pre-polarimeter optics must generate <2% crosstalk between polarization states (goal <1%);

★ the instrument must provide spectra w/ S/N~100 per ~2 km/s pixel in 1 hr @ J=12 & K=11; the instrument must also be capable of observing stars with H magnitudes in the range 1 (bright limit) down to 14 (faint limit);

★ the instrument must ensure an observational efficiency of >70% and >90% for 15-min and 1-hr exposures respectively, to guarantee high-enough observing duty cycles on large survey programs;

★ the instrument must be able to access all stars up to a zenithal distance of 70° (corresponding to an airmass of 2.5).

We include below a matrix emphasizing how critically the various science objectives relate on the various science specifications. The science objectives are referenced through their section numbers, i.e. **3: exoplanets of low-mass dwarfs**, **4: stellar formation & magnetic fields**, 5: other programs in stellar physics, 6: planetary atmospheres, 7: galactic/extragalactic astronomy.

9. SPIRou: a niche of excellence

As shown above, SPIRou can efficiently tackle a wide range of front-line science cases and shows up as a very attractive option. In addition, there is **no existing instrument worldwide providing similar capabilities & performances** yet and very few (if any) are expected to show up in the coming 5 yr, making SPIRou even more interesting & perfectly timely.

9.1. Optimal performances

The majority of the existing nIR spectrographs on large telescopes and featuring high-resolution modes provides no more than a very limited simultaneous spectral coverage - at most a few % of the domain central wavelength, e.g.,:

instrument / telescope	resolving power	slit width (")	domain (µm)	single-shot coverage (λ)
NIRSPEC / KECK2	25 K	0.43	0.95-5	1.5%
IRCS / SUBARU	20 K	0.14	0.95-5.5	2.5%
CRIRES / VLT	20-100 K	1-0.2	1-5	1.4%

Moreover, only few existing or planned high-resolution spectrographs on >3m-class telescopes will provide a large simultaneous coverage of the nIR domain:

instrument / telescope	resolving power	aperture (")	domain (µm)	year
GIANO / TNG	25-50 K	fibre / 0.6	0.92-2.35	2012
CARMENES / CA	82 K	fiber / 1.5	0.90-1.7	2015
IRD / SUBARU	70 K	fiber / 1.5	1.2-1.8	2015
SPIRou	**75 K**	**fiber / 1.3**	**0.98-2.35**	**2017**
HPF / HET	50 K	fiber / 1.7	0.85-1.7	>2017

Among those, only GIANO is on the telescope (first light in 2012 July), although no science runs has been allocated yet (at least until early 2014). Both CARMENES on Calar Alto and IRD on SUBARU are in construction, with a first light currently scheduled for 2015; however, while CARMENES may only operate for a few years (until Calar Alto's likely shutdown in 2018), IRD on SUBARU is unlikely to be allocated the hundreds of nights that an ambitious RV survey of M dwarfs requires (given the oversubscription rates typical to 8m-class telescopes). HPF on the Hobby-Eberly Telescope is only partly funded at the moment, and, if constructed, is likely to suffer from the same drawbacks as IRD.

SPIRou is thus a unique instrument in this context. With the K band, it will provide a major increase in RV efficiency (see Sec 8.1 & Fig 8.1) **as well as a window to embedded protostars** (see Sec 4); **it will also implement polarimetric capabilities, and therefore ways to investigate magnetic fields of protostars and to model / filter out activity jitters plaguing RV curves.** With the specifications listed in Sec 8.7, **SPIRou appears as the most attractive & ambitious instrument of its class**, providing unique opportunities & optimal performances for carrying out a wide range of front-line science programs. In particular, **SPIRou is ideally phased**

with space-based instruments with ambitious exoplanet science programs like TESS/NASA, CHEOPS/ESA (both scheduled for 2017) **and JWST/NASA** (2018) that will require intensive ground observations / follow-ups - both to confirm the exoplanet candidates detected with photometric surveys and to identify the transiting habitable exoEarths whose atmosphere will be scrutinized for the presence of biomarkers (see Sec. 6.3). PLATO/ESA is scheduled for 2024 and will also require intensive follow up which could be an essential program for SPIRou, 7 years after its implementation.

9.2. Worldwide coordinated science

The various science programs described in Sec 3-7, and in particular the search for habitable exoEarths, require a very large amount of observing time - potentially a large fraction of the full observing capability of CFHT. This amount of observing time can only be realistically granted in the framework of large-scale international collaborations (including in particular the main experts in the fields), like, e.g., the MagIcS worldwide initiative aimed at exploring stellar magnetic fields across the HR diagram (using in particular ESPaDOnS/CFHT).

By gathering many famous contributors both from within and from outside the CFHT community, the SPIRou science group (see Appendix A) already reflects this collaborative action. If SPIRou is funded, the science group will grow and fork into several SPIRou science teams while the instrument is being designed, constructed and commissioned - each team taking care of optimizing program outlines & sample selections for specific science topics; regular coordination between science teams will ensure in particular that sample overlaps between programs are properly managed with the goal of maximizing the overall scientific return. Ultimately, these science teams will be in charge of submitting Large Programs (LPs) to CFHT time allocation committees (TACs) to be granted the large amount of observing nights that they will require.

9.3. The SPIRou Legacy Survey

Obviously, the amount of observing time required to complete the various science programs outlined above is large, with already 1,300+ nights needed to cover the two main science goals. In this context, **SPIRou only makes sense if coupled to the allocation of a guaranteed SPIRou Legacy Survey of 500 CFHT nights on a timescale of ~5 yr, allowing in particular to complete the discovery phases of the large surveys proposed on both main science programs** (see Sec 3 and 4).

More specifically, the SPIRou Legacy Survey will be divided into 3 main components. Two of them will be dedicated to exoplanets, respectively focussing on (i) a RV survey of the ~60% closest M dwarfs in each mass bin of our sample (requiring 300 nights), and (ii) a follow-up of the transiting planet candidates (to be discovered by TESS/NASA) with smallest radii and orbits closest to their HZs (75 nights). The third survey component will concentrate on star/planet formation, and more specifically on large-scale magnetic fields and young hot Jupiters of class-I-III protostars in the Taurus/Auriga, ρ Oph and TWA star-forming regions (125 nights). The SPIRou Legacy Survey is expected to unveil a wealth of new worlds, many of which habitable, and to yield forefront discoveries on the origins of Sun-like stars and Earth-like planets. It will come as a reward for the consortium members participating to the funding of the instrument.

All other programs with SPIRou will take the form of PI proposals or LPs, and will come as a complement / follow-up to the Legacy Survey for both main science goals

9.4. Queue service observing (QSO)

Once the SPIRou Legacy Survey, LPs and PI programs are granted time, observing with SPIRou will be carried out through the QSO mode. Coordinators from the SPIRou science group will remotely follow data acquisition in near-real time to confirm that the collected spectra are of nominal quality for the need of the various science programs, as is routinely done today in the case of ESPaDOnS.

10. Summary & conclusions

The present document lists all fore-front science programs that SPIRou - the nIR spectropolarimeter proposed as a new generation instrument for CFHT - can carry out, with particular emphasis on the key ones for which SPIRou is expected to be world-leader : hunting for & characterizing habitable exo-Earths around low-mass dwarfs (Sec 3) and investigating magnetized star/planet formation (Sec 4). Other exciting science programs for SPIRou are numerous, including dynamo processes in fully-convective dwarfs, weather patterns on brown dwarfs (Sec 5), atmospheres of solar-system planets and stellar archeology in the Milky Way (Secs 6-7).

The science specifications needed to carry out these programs as successfully & efficiently as possible are also mentioned (Sec 8), addressing in particular critical issues such as the required wavelength domain, resolving power, RV precision, polarimetric capabilities & instrument sensitivity (see Sec 8.7 for a summarizing list). A comparison with similar existing or planned facilities (Sec 9) shows that **SPIRou will not only fill a niche but will be quite unique**, granting the CFHT community with plenty of new results & major breakthroughs in multiple research fields. Moreover, SPIRou will be **ideally phased with space-based instruments like TESS/NASA, CHEOPS/ESA** (both scheduled for 2017) **and JWST/NASA** (2018), whose success will critically depend on ground-based RV surveys like the one we propose to carry out with SPIRou.

This document demonstrates that SPIRou will be optimally suited for pioneering several extremely popular astrophysical research fields. SPIRou indeed ideally matches the conclusions of many research agencies worldwide. In USA, the NRC 2010 decadal survey in Astronomy & Astrophysics states that one of the top three scientific objectives is «New Worlds: Seeking Nearby, Habitable Planets», recommending to undergo **«an aggressive program of ground-based high-precision RV surveys of nearby stars to identify potential candidates»**; similarly, in France, the CNRS / INSU 2009 prospective concludes that «SPIRou is the most promising solution for the CFHT beyond 2015, well suited in particular to the scientific needs of the French community, and thus appears as the top priority among mid-size, mid-term equipments».

As a conclusion, SPIRou will ensure that **CFHT remains a top-class facility until at least 2020** as a key actor in observational astrophysics.

Appendix A : the SPIRou science group

Below is a list of people with explicit interest in SPIRou & associated science goals. In addition to people in the **core team** (including those strongly involved in the instrument definition), we list contributors (who participated in the writing of the science case) & supporters (who declared their interest for the instrument). Contributors to the exoplanet (Sec 3), stellar formation (Sec 4) & other science drivers (Secs 5-7) are shown in pink, green & blue respectively.

Community	Institute / Country	**Core team**	Contributors	Supporters
France	IRAP / Toulouse	**Donati**	Jouve Joblin	Ferrière Dintrans Baruteau Petit Fouqué
	IPAG / Grenoble	**Delfosse Bonfils**	Bouvier Forveille Ménard Barthélémy	Dougados Delorme Lilensten
	LAM / OHP / Marseille	**Bouchy Moutou**	Boisse	Deleuil Bouret
	SaP CEA / Saclay		Brun Hennebelle	Mathis Fromang
	LESIA / Meudon		Widemann	Bézard Lellouch Doressoundiram Fouchet Zarka Coudé du Foresto
	LUTH / Meudon			Zahn Mazevet
	OCA / Nice		deLaverny Recio-Blanco	Guillot Hill
	ENS / Lyon		Chabrier	Allard
	ENS / LERMA / Paris			Dormy Petitdemange Cabrit
	GRAAL / Montpellier		Morin Martins	Lèbre
	IAP / Paris	Hébrard		Lecavelier, Terquem
	IAS / Orsay			Ollivier Bordé Baudin
	UTINAM / Besançon		Reylé	
	LATMOS / Paris			Leblanc
	IMCCE / Paris			Laskar Boué
Canada	UdeM / Montréal	Doyon Artigau		Lafrenière StLouis Bastien Moffat Dufour
	UofT / Toronto			Jayawardhana
	McMaster / Toronto			Pudritz
	UWO / London		Houde	Metchev
	UBC / Vancouver			Matthews
	NRC / Victoria			Marois Bohlender
	UVic / Victoria			Ven
	RMC / Kingston			Wade
Taiwan	ASIAA / Taipei	**Wang**	Takami	Lai
Brazil	UFMG+UFRN+USP +ON	**Alencar Diaz**		Martioli Castilho
Others	Switzerland	Pepe Udry		Lovis
	Portugal	Figueira		Santerne Santos

Community	Institute / Country	**Core team**	Contributors	Supporters
	Italy		Flaccomio	Argiroffi, Baffa
	UK		Gregory Jardine	Cameron Harries Barnes Baraffe Browning Mohanty
	USA		Romanova	Valenti Feigelson Toomre Shkolnik
	ESO		Hussain	
	Australia		Marsden	Carter

Appendix B : Observing time vs science objectives

We summarize below the estimated number of nights[6] needed to address with reasonable completeness all various scientific programs described in Sec 3-7 (and referred to with their respective section number). In case of sample overlaps between programs, we only list in Col 3 the time that has not been counted already.

We also outline in Col 4 the number of nights we ask CFHT in the framework of the SPIRou Legacy Survey (see Sec 9.3)**, which corresponds to the «discovery phase» of our 2 main science programs, i.e., the SPIRou planet search** (see Sec 3) **and the SPIRou magnetized star/planet formation program** (see Sec 4)**.**

Sect	title	full program	Legacy Survey	comments
3.2	follow-up of transiting planet candidates	**150**	**75**	150 ★ & 60 visits/★
3.2	RV survey of M dwarfs	**600**	**300**	600 ★ & 60 visits/★
3.4	exoplanet statistics	**250**		350 ★ & 40 visits/★
3.5	giant planets / ultra-cool dwarfs	**75**		100 ★ & 20 visits/★
4.3	magnetic fields of protostars & magnetospheric accretion models	**250**	**125**	250 ★ & 20 visits/★
4.4	magnetic fields of gaseous accretion discs	**50**		10 ★ & 40 visits/★
4.5	planet formation			full sample overlap w/ 4.3 & 4.4
5.1	dynamo processes in red & brown dwarfs	**50**		100 ★ & 10 visits/★ sample overlap w/ 3.2 & 3.5
5.2	weather patterns on brown dwarfs	**30**		10 ★ & 24 visits/★
5.3	cool magnetic spots on active stars	**25**		20 ★ & 10 visits/★
5.4	ultra-cool spectroscopic binaries & the formation of brown dwarfs			100 ★ & 10 visits/★ full sample overlap w/ 3.5
5.5	formation of massive stars	**10**		80 ★
5.6	circumstellar environments	**10**		
6 & 7	planets & galaxies	**50**		
		~1500	**500**	

The grand total yields ~1500 nights, with **500 nights making the SPIRou Legacy Survey** outlined in Sec 9.3.

[6] Throughout the whole document, observing times are counted as CFHT QSO nights, i.e., clear observing time counted at an average rate of 8 hr/night (as in the case of, e.g., ESPaDOnS).

Appendix C : On the habitability of exoplanets

Two limitations regarding the habitability of planets around M dwarfs are regularly invoked, but recent studies argue that none is apparently fatal (see Horner & Jones 2010, IJAsB 9, 273, for a review).

Firstly, M-dwarfs are know to have strong chromospheric activity and in particular to be the source of flares emitting UV radiation that may induce DNA destruction. However, even a modest atmosphere of an oxygen rich exo-Earth protects the biosphere from UV radiations of active M-dwarfs (Heath et al 1999, Origins of Life & Evolution of the Biosphere 29, 405) : «UV radiation goes into photolyzing ozone in the atmosphere, preventing it from reaching the planetary surface (Segura et al 2010, AsBio 10, 751)».

Secondly, planets in the habitable zone of M-dwarfs are close to their stars, and thus subject to intense tidal force which are supposed to synchronize the planetary spin with the orbital period. The strong permanent illumination gradients may induce freezing of water in the dark side and evaporation on the illuminated side. However some studies finding that an ocean on the dark hemisphere does not systematically freeze : greenhouse effects on a modest atmosphere (a tenth of that of the Earth) could sufficiently redistribute the energy between the two sides (Heath et al. 1999; Origins of Life & Evolution of the Biosphere, 29, 405). Perhaps as important, our solar system provides counter-examples of planets exposed to strong tidal forces, and which are not tidally synchronized: tidal interactions did capture Mercury into a spin-orbit resonance 3/2 rather than 1/1, and Mercury is not synchronized. The capture probability in spin-orbit resonances other than 1/1 vastly increases for large eccentricities as well as for systems that are not at present in an high eccentric state but that may have gone through a high eccentric state in the past (Correia & Laskar 2004, Nature 429, 848 & 2010 Icar 205, 338).

A more detailed and up-to-date account on these issues (as well as a discussion of several other effects potentially affecting habitability of planets around M dwarfs) can be found in Delfosse et al 2013 (A&A 553, 8).